

Auxiliary Material Submission for Paper 2013GL055786

Noble Gas Composition in Rainwater and Associated Weather Patterns

Rohit B. Warriar¹, M. Clara Castro¹, Chris Michael Hall¹ and Kyger Lohmann¹
(¹University of Michigan, Department of Earth and Environmental Sciences, 1100 N.
University Ave., Ann Arbor, MI 48109-1063, USA)

Introduction

This file compiles all supplementary material for the manuscript titled “Noble Gas Composition in Rainwater and Associated Weather Patterns”. Specifically, sample location map of southern Michigan (Supplementary Figure 1: page 43), mean climate summary for Ann Arbor, MI (Supplementary Figure 2, page 44) along with measured noble concentrations and Helium isotope ratios (Supplementary Table 1, page 39). Detailed weather data description for individual rainfall events collected in this study is presented in Supplementary Text 1 (page 5) along with hourly surface weather station observations (Supplementary Table 2, page 40). In addition, various weather data products including area forecast discussions for samples nr1, 2, 6 and 12 (Supplementary Text 2, page 11), surface analysis maps for nr1, 6, 10 (Supplementary figures 3-5, page 45-47), Doppler radar image for nr2 (Supplementary figure 6, page 48), SkewT-log P plot of weather balloon measurements for samples nr1, 6, 11 and 12 (Supplementary figure 7, page 49) and surface weather observations (Supplementary figure 8, page 50) are provided.

In addition, Supplementary Text 3 (page 26) discusses in detail diffusive mass transfer of noble gases in a raindrop assuming various boundary conditions and diffusion coefficients (Supplementary Table 3, page 41) along with a description of raindrop size estimation. Results of time-dependent diffusive mass transfer of noble gases in a raindrop are shown in supplementary figures 9 and 10 (page 51-52) while results of raindrop size estimation are presented in Supplementary Table 4 (page 42) along with a plot of terminal velocity as a function of raindrop size (Supplementary figure 11, page 53) and a plot of noble gas diffusive equilibrium in a raindrop of radius 0.1mm and 5mm (Supplementary figure 12, page 54). In addition, calculation of the time taken for measured noble gas disequilibrium patterns in rainfall to re-equilibrate at the surface is provided in Supplementary Text 4 (page 35).

For higher resolution figures, the reader is referred to individual figure files placed in the supplementary material. Below, supplementary files included in this manuscript are listed along with a table of contents.

Supplementary File Index:

1. Supplementary Text

- 1.1. Supplementary Text 1:** Detailed weather data description for individual rainwater samples.
- 1.2. Supplementary Text 2:** Area forecast discussions for southeast Michigan corresponding to samples nr1, 2, 6 and 12.

- 1.3. **Supplementary Text 3:** Diffusive Mass Transfer of noble gases in a Raindrop and calculation of average raindrop sizes from measured noble gases in rainwater
- 1.4. **Supplementary Text 4:** Time taken for noble gas disequilibrium patterns in rainfall to re-equilibrate at the surface

2. Supplementary Tables

- 2.1. **Supplementary Table 1:** Rainwater sampling location, date and time of collection, measured surface air temperature (T), noble gas concentrations and measured He isotopic ratios (R) normalized to atmospheric He ratio (R_a). Samples from Milan and Ann Arbor were collected at altitudes of 215m and 290m a.s.l respectively. Surface weather station records used to derive appropriate precipitation characteristics for corresponding rainfall event is also indicated.
- 2.2. **Supplementary Table 2:** Compiled hourly surface weather observations from individual weather station records. Data description for each column in Table S2 including units, abbreviations and weather codes are provided in detail by NCDC (<http://hurricane.ncdc.noaa.gov/cdo/3505doc.txt>).
- 2.3. **Supplementary Table 3:** Noble gas diffusion coefficients in ice and liquid water.
- 2.4. **Supplementary Table 4:** Estimated condensation altitudes and raindrop sizes for individual precipitation events corresponding to mass-dependent samples based on diffusive mass-transfer model.

3. Supplementary Figures

- 3.1. **Supplementary Figure 1:** (a) Location of Michigan and (b) rainwater sample collection sites in Ann Arbor and Milan. Base map and locations are obtained through map services from U.S. Geological Survey, National Geospatial Program (<http://nationalmap.gov/>).
- 3.2. **Supplementary Figure 2:** 1981-2010 Mean climatological summary for Ann Arbor (Station ID: USC00200230; 42.28°N, 83.77°W) located in southeast Michigan (a) Monthly mean total precipitation and (b) monthly mean maximum, minimum and average temperatures.
- 3.3. **Supplementary Figure 3:** Surface analyses map of North America issued by the Hydrometeorological Prediction Center corresponding to nr1 precipitation event.
- 3.4. **Supplementary Figure 4:** Surface analyses map of North America issued by the Hydrometeorological Prediction Center corresponding to nr6 precipitation events.
- 3.5. **Supplementary Figure 5:** Surface analyses map of North America issued by the Hydrometeorological Prediction Center corresponding to nr10-1/10-2 precipitation event.
- 3.6. **Supplementary Figure 6:** Doppler radar (NEXRAD) image for southeast Michigan at 00:25 UTC on July 4th, 2011. Location of hourly surface weather stations near Ann Arbor and Milan are also indicated (orange circles).
- 3.7. **Supplementary Figure 7:** SkewT-log P plot of weather balloon measurements of temperature and dew point at Detroit, MI for samples nr1, 6, 11 and 12.
- 3.8. **Supplementary Figure 8:** Plot of surface pressure, temperature, dew point and cloud ceiling height measurements for samples nr1 and nr12 measured at Ann Arbor and Custer weather stations respectively.

- 3.9. Supplementary Figure 9:** Comparison of measured rainwater noble gas patterns for sample nr4-2 (black markers) with the time dependent evolution of noble gas patterns within a raindrop of size 5mm starting from ice (green triangles). **(a)** Model noble gas patterns in a raindrop for various time 't' derived by assuming a constant equilibrium boundary condition and diffusion coefficients for ice (red markers) and liquid water (blue markers). Shaded region indicates domain of model rainwater patterns for t=1000s; **(b)** Model noble gas patterns in raindrop for various time 't' (green dashed lines) derived by assuming variable equilibrium boundary conditions (red dots) and liquid water noble gas diffusion coefficients.
- 3.10. Supplementary Figure 10:** Comparison of the time evolution of noble gases within a raindrop of size 5mm derived by assuming boundary conditions and diffusion coefficients investigated in sections 2-4 of supplementary text3. These include (1) a constant equilibrium boundary condition of ASW at 0°C and noble gas diffusion coefficients in ice (green line); (2) constant equilibrium boundary condition of ASW at 0°C and noble gas diffusion coefficients in liquid water (red line); (3) varying equilibrium boundary condition as well as liquid water noble gas diffusion coefficients (blue line).
- 3.11. Supplementary Figure 11:** Terminal velocity of raindrops as a function of droplet size assuming multiple formulations.
- 3.12. Supplementary Figure 12:** Time taken for noble gases to achieve diffusive equilibrium through mass transfer in/out of a raindrop of radius 0.1mm and 5mm.

Table of Contents

S.No.	Supplementary File	Page no.
1	Supplementary text 1	5
2	Supplementary text 2	11
3	Supplementary text 3	26
4	Supplementary text 4	35
5	Table S1	39
6	Table S2	40
7	Table S3	41
8	Table S4	42
9	Figure S1	43
10	Figure S2	44
11	Figure S3	45
12	Figure S4	46
13	Figure S5	47
14	Figure S6	48
15	Figure S7	49
16	Figure S8	50
17	Figure S9	51
18	Figure S10	52
19	Figure S11	53
20	Figure S12	54

Supplementary Text 1: Detailed weather data description for individual samples

1. Introduction to weather products

For each of the precipitation events associated with our sampling collection multiple weather products were analyzed to provide a detailed characterization of each one of these events. Detailed weather information for each sample include: a) synoptic scale weather patterns such as movement of cold/warm fronts and location of high/low pressure ridges/troughs; b) precipitation characteristics such as rainfall intensity (light, moderate, heavy rainfall), presence or absence of thunder, hail, fog; and c) probable condensation altitudes.

Synoptic scale weather features were obtained using surface analyses maps based on station observations issued every three hours by the Hydrometeorological Prediction Center (archived at http://www.hpc.ncep.noaa.gov/html/sfc_archive.shtml). Figures S3, S4 and S5 show examples of such maps corresponding to rainfall events during collection of samples nr1, 6, and the two samples 10-1 and 10-2. Similar maps are used to describe weather features in detail for each rainfall event during collection of all samples (cf., section 2 below). Description of various fronts and boundaries shown on the maps are available at the National Weather Service glossary (<http://www.nws.noaa.gov/glossary/>). Synoptic scale weather pattern descriptions obtained through surface analysis maps were crosschecked with area forecast discussions issued by the National Weather Service for the Detroit/Pontiac region (archived at <http://mesonet.agron.iastate.edu/wx/afos/list.phtml>). Text S2 provides examples of unedited area forecast discussions that are most up to date prior to precipitation events of samples nr1, 2, 6 and 12. Precipitation characteristics for each sampling event were derived from available surface weather station observations. All weather station records were obtained from the Integrated Surface Hourly database published by the National Climatic Data Center (NCDC; <http://gis.ncdc.noaa.gov/web/ish.html>). Because an hourly weather station is not available in Milan, MI, the closest available weather stations (cf. Fig. S6) located in Ann Arbor (~15 kms; NCDC WBAN station number: 725374), Willow Run (~19 kms; NCDC WBAN station number: 725376) and Custer (~27 kms; NCDC WBAN station number: 725418) were used to derive precipitation characteristics in Milan. Individual weather station records used for each sampling event are shown in Table S1. All weather records relevant to a particular precipitation event are included in Table S2. Data description for each column in Table S2 including units, abbreviations and weather codes are provided in detail by NCDC (<http://hurricane.ncdc.noaa.gov/cdo/3505doc.txt>). It should be noted that weather data from a particular weather station was utilized only after ensuring that the specific storm passed through both the sampling location and appropriate weather station at the precise time of sampling by analyzing archived Doppler radar images (available every 5 minutes) for southeast Michigan (NEXRAD available at <http://www.ncdc.noaa.gov/oa/radar/radarresources.html>). Figure S6 shows an example of a Doppler radar image for the precipitation event during collection of sample nr2. Similar images were obtained for all other samples using the same archive. Condensation altitudes for each sample were estimated from available weather balloon (sounding) data at Detroit, MI (42.695°N, -83.467°W; Fig. S1). Similar to weather station records, sounding data from Detroit for a particular rain event was utilized only after ensuring that the specific storm

passed through both the sampling location and Detroit (~80 kms and ~70 kms from Milan and Ann Arbor, MI, respectively) at the precise time of sampling by analyzing archived Doppler radar images for southeast Michigan. Sounding data is available twice daily (at 0 and 12 UTC (Coordinated Universal Time)) from the NOAA/ESRL Radiosonde database (esrl.noaa.gov/raobs) and is plotted in the form of SkewT-logP plots (<http://RUCsoundings.noaa.gov>), which is a vertical snapshot of temperature, dew point and winds above a point on Earth. Further information about radiosonde (weather balloon) data and SkewT-log P plots is available at the Federal Meteorological handbook at www.ofcm.gov/fmh3/text/default.htm. Figure S7 shows examples of SkewT-log P plots corresponding to samples nr1, 6, 11 and 12. Probable condensation altitudes can be estimated as those altitudes in the SkewT-log P plot at which measured temperature (red lines, Fig. S7) is similar to the dew point (blue line, Fig. S7). This is discussed in detail in section 2.

Weather data descriptions obtained by simultaneously analyzing all the above weather products for individual rain events during collection of each sample are provided below. As mentioned above, weather products are available only at specific hours that may or may not necessarily correspond to the precise time of our sampling event (Table S1). However, weather descriptions provided below utilize the most recently available weather products prior to the sampling event and represents our best attempt at describing the weather patterns at the time of sampling. Nevertheless, synoptic weather patterns and precipitation characteristics collectively derived clearly seem to differ vastly between mass independent (nr1, 8, 12, 14) and mass dependent samples as described below. A brief summary comparing the distinct weather patterns observed for mass dependent and mass-independent samples is also provided (Section 4).

2. Detailed description of weather information for Mass-Independent samples

2.1 Sample nr1

The surface analysis map (Fig. S3) indicates the presence of a low-pressure trough in the Ohio valley producing precipitation in southeast Michigan. Similar synoptic scale weather patterns were identified in the area forecast discussion (cf. Text S2). Surface weather records at Ann Arbor indicate the presence of mist/fog, light to moderate rain and low cloud ceiling heights (~300m) through both manual and automated observations between 15:12 UTC and 15:53 UTC when the sample was collected (Table S2, Figure S8). Available temperature and dew point sounding at 12 UTC visualized in the SkewT-log P plot (Fig. S7) indicates that condensation can occur between ~300m and ~3kms (1000ft and 10,000ft) and probably at higher altitudes (e.g., 3.6kms or ~12,000ft) where air temperatures are below 0°C. This suggests that in addition to the low clouds/fog observed through surface observations, condensation originating as ice/ice melt from higher condensation altitudes are definitely likely.

2.2 Sample nr8

The surface analysis map at 18 UTC indicates the presence of a low-pressure trough across the lower peninsula of Michigan. Between 18:34 UTC and 19:34 UTC when nr8 was collected, surface weather observations at Custer weather station indicates the presence of intermittent rain and mist (cf. Table S2). The presence of fog/mist and low altitude clouds

was also predicted in the area forecast discussion. SkewT-log P plots of temperature and dew point sounding data at 12 UTC and 24 UTC on August 6th, 2011 indicates the probability of multiple condensation levels in addition to the presence of low altitude clouds. Some of these condensation levels occur at altitudes where temperatures are below 0°C suggesting that condensation originating as ice/ice melt are likely.

2.3 Sample nr12

Area forecast discussion and surface analyses maps at 6 UTC and 9 UTC show that precipitation collected at 7:50 UTC is associated with an upper level low pressure system ahead of a warm front moving in to southern Michigan from the southwest. Surface weather station at Custer observed light continuous rain at 7:53 UTC. While the presence of fog was not reported at this weather station, area forecast discussions had predicted the presence of fog (cf. Text S2). In addition, surface temperature and dew points were the same during the period of sample collection indicating the presence of low-altitude clouds/fog (cf. Fig. S8). SkewT-log P plots of temperature and dew point sounding data at 0 UTC and 12 UTC also indicate that low altitude clouds are likely (cf. Fig. S7). In addition, SkewT-log P plots also indicate condensation levels at higher altitudes (~4.5 kms or ~15,000 ft) where temperatures are below 0°C suggesting that condensation originating as ice/ice melt is likely.

2.4 Sample nr14

Similar to other samples with mass-independent patterns, both the surface analysis map at 15 UTC and the area forecast discussion suggest that this precipitation event was due to the presence of a low pressure trough south of Michigan in the Ohio Valley. Surface weather records at the Ann Arbor weather station at 15:10 UTC indicates continuous, moderate rain with the presence of mist identified both manually and through automated observations. Low cloud ceiling heights (less than 300m) were observed at the Ann Arbor weather station and previously predicted in the area forecast discussions. However, sounding data is not available for this precipitation event because NEXRAD images do not indicate that the storm passed through both Detroit and Milan at the time of sample collection. Thus, likely condensation altitudes could not be predicted for this sample.

3. Detailed description of weather for mass dependent samples

3.1 Sample nr2

Area forecast discussion and NEXRAD images (Fig. S6) for this precipitation event indicate the occurrence of an isolated thunderstorm due to lake breeze interactions. This isolated thunderstorm misses all available weather stations at the time of sample collection (Fig. S6). Thus, precipitation characteristics and condensation altitudes could not be derived for this sample.

3.2 Samples nr3-1, nr3-2 and nr4-1, nr4-2

Area forecast discussions predict the occurrence of thunderstorm clusters during the eastward movement of a mesoscale convective complex across southern Michigan during sample collection of nr3-1, 3-2 followed by a second upper level disturbance igniting

additional thundershowers during collection of nr4-1, 4-2. While the storm passes through Custer weather station, cloud ceiling height and precipitation characteristics observations were not recorded during the time of sample collection of nr3-1, -2 (cf. Table S1, S2). However, during sample collection of nr4-1, 4-2, the Ann Arbor weather station (cf. Table S2), through which the storm passes, recorded moderate to heavy rain with showers of hail between 21:53 UTC and 22:05 UTC. In addition, SkewT-log P plot at 0 UTC corresponding to nr4-1, 4-2 suggest the presence of multiple condensation levels including at altitude of ~4.5km (~15,000 ft) where temperatures are below 0°C suggesting that condensation originating as ice/ice melt is likely.

3.3 Samples nr5-1 and nr5-2

Surface analyses and area forecast discussions indicate initially a stationary front followed by an advancing warm front that moves east from northern Illinois to southern Michigan bringing with it a thunderstorm complex. Precipitation characteristics recorded at the Ann Arbor weather station initially indicate continuous, moderate rain and mist followed by heavy rain, thunderstorms and hail showers (Table S2). The heavy rain is also captured by the Doppler radar images for these precipitation events. SkewT-log P plot created with temperature and dew point measurements from weather balloons at 0 UTC on July 28th, 2011 indicate that condensation altitudes up to ~4.5kms (~15000 ft) are likely. Because temperatures are ~0°C at these altitudes, condensation originating as ice/ice melt is probable.

3.4 Sample nr6

Both the surface analysis map (Fig. S4) and area forecast discussion suggest that this precipitation event occurs due to convection along a stationary front that is positioned in a southwest-northeast direction across the lower peninsula of Michigan. Area forecast discussions further suggest the likelihood of numerous thunderstorms in southeast Michigan. Indeed, surface weather observation at Ann Arbor indicates moderate to heavy rain with showers of hail between 8:13 UTC and 8:51 UTC when sample nr6 was collected (Table S2). In addition, SkewT-log P plot at 0 UTC and 12 UTC (Fig. S7) suggest the presence of multiple condensation levels including altitudes of 1.2km, 2.1km, 4.5km and 6km (or 4000ft, 7000ft, ~15,000ft and 20,000ft). Measured temperatures are below 0°C above ~4.5 km (red line, Fig. S7) suggesting that condensation originating as ice/ice melt is likely.

3.5 Sample nr7

Surface analysis and area forecast discussions suggest heavy rainfall and thunderstorms produced by instability in southern Michigan as indicated by a stationary front. The presence of heavy rain at the time of sample collection is also indicated by Doppler radar images and confirmed by surface weather observations at the Ann Arbor weather station which record heavy rain with hail showers at 7:13 UTC, close to the sample collection instant (Table S2). In addition, cloud base heights recorded at these very same surface weather stations are high (between 1.2km and 2.4km or 4200ft and 8000ft) and suggest multiple condensation levels. Multiple condensation levels at ~1.5km, 3km, 4.5km and 5.4km (or 5000ft, 10,000ft, 15,000ft and 18,000ft) are also evident through SkewT-log P

plots at 0 UTC. Condensation at altitudes higher than ~4.5kms where temperatures are below 0°C suggest that precipitation originating as ice/ice melt is likely.

3.6 Samples nr9 and nr10-1, 10-2

Surface analysis indicates the movement of a warm front across southern Michigan in a northeast direction producing strong upper level moisture advection generating heavy rain and thunderstorms as also described in the area forecast discussions for nr9. This is followed by a cold front associated with a low pressure system over Ontario, which sweeps across southern Michigan from west to east bringing with it showers and thunderstorms during which nr10-1 and 10-2 are collected (Fig. S5). Surface weather observations in Ann Arbor also indicate moderate to heavy rainfall with thunderstorms and hail showers between 9:33 UTC and 9:36 UTC when nr9 was collected (Table S2). While thunder with rain is reported in the surface analysis map ahead of the cold front during nr10-1 and nr10-2 sample collection, surface weather data is not available at Willow Run station, through which this particular storm passes, to confirm this. However, we have physically observed thunderstorms and hail during sample collection of nr10-1 and 10-2. In addition, we observed a significant drop in temperature (2.8°C) at the collection site between sampling of 10-1 and 10-2 suggesting that the cold front passed through Milan during that time interval. Sounding plots for both samples indicate multiple condensation level where temperatures are below 0°C and suggests the likelihood of precipitation originating as ice/ice melt.

3.7 Sample nr11

Surface analysis map indicates a stationary front slowly moving across southern Michigan from north to south associated with a mid level storm rotating across northern Ohio bringing with it rain and thunderstorms as indicated in the area forecast discussion. Surface weather station at Ann Arbor does not report any particular precipitation characteristic during sample collection (Table S2). Similar to all other samples, multiple condensation levels below 0°C are possible as indicated by SkewT-log P plots (Fig. S7) suggesting the likelihood of precipitation starting as ice.

3.8 Sample nr13

Surface analyses maps indicate a stationary front positioned across southern Michigan, which then moves as a cold front across the Lower Peninsula. Area forecast discussion indicates that this will bring clusters of thunderstorms to southeast Michigan. These are confirmed by surface weather observations at Ann Arbor, which record heavy rain, thunderstorms and showers of hail (Table S2). In addition, sounding plots point to multiple condensation levels and the presence of condensation altitudes below 0°C.

4. Summary of weather analyses for mass-independent and mass-dependent samples

Our detailed weather analyses above indicate that all rain samples with mass-independent patterns were collected during precipitation due to the presence of a low-pressure system in the area. Weather records for all samples with mass-independent patterns, without exception,

indicate that corresponding precipitation events can be characterized by the presence of fog/mist, light to moderate rain and low cloud ceiling heights (~300m). By contrast, samples with mass-dependent patterns were collected during energetic thunderstorms due either to a stationary front (e.g., nr6), cold front (e.g., nr10-1/10-2) or warm front (e.g., nr9). Surface weather stations confirm this by recording heavy rain, thunderstorms and showers of hail during the time of sample collection. Of particular significance, is the fact that except for some initial fog activity during the approach of the thunderstorm during collection of sample nr5-1, no other surface weather station records the presence of fog or low-level clouds during collection of mass-dependent samples. In addition, all samples, including those displaying mass-dependent and mass-independent patterns indicate the possibility of multiple condensation levels, including altitudes where air temperature is below 0°C. These results suggest the likelihood of precipitation starting as ice in southeast Michigan, a finding that was also previously suggested by *Bernstein et al.* [2007].

References

- Bernstein, B. C., Wolff, C. A., & McDonough, F. (2007). An Inferred Climatology of Icing Conditions Aloft, Including Supercooled Large Drops. Part I: Canada and the Continental United States. *Journal of Applied Meteorology and Climatology*, 46(11), 1857–1878. doi:10.1175/2007JAMC1607.1

Supplementary Text 2: Area forecast discussions for southeast Michigan corresponding to samples nr1, 2, 6 and 12

1. Introduction

Area forecast discussions (AFDs) provide information on synoptic and mesoscale weather features at the local region where the issuing weather station is located. This supplementary text collates unedited AFDs for southeast Michigan region issued by the National Weather Service in Detroit/Pontiac, MI (archived at <http://mesonet.agron.iastate.edu/wx/afos/list.phtml>). Because multiple AFDs are issued every day, only the most recent and up-to-date AFD prior to the date and time of rainwater sample collection are included here. For example, on May 15 2011 nr1 was sampled at 15:40 UTC (Coordinated Universal Time). AFDs were issued by the National Weather Service in Detroit/Pontiac at 1:34, 4:50, 7:30, 10:59, 17:24, 18:47 and 23:00 UTC. AFD included in this Supplementary Text corresponds to 10:59 UTC (6:59 AM, EDT) since it is the most up-to-date AFD prior to the occurrence of precipitation event nr1 sampled in this study. Below, we only include AFDs for a few samples (nr1, 2, 6 and 12) for demonstrative purposes. AFDs for all remaining samples are available at the National Weather Service archive listed above.

2. Sample Area Forecast Discussions

2.1 Sample nr1

480 FXUS63 KDTX 151059 AFDDTX AREA FORECAST DISCUSSION NATIONAL WEATHER SERVICE DETROIT/PONTIAC MI 659 AM EDT SUN MAY 15 2011

.AVIATION...

WIDESPREAD IFR BASED STRATUS WILL START THE TAF PERIOD AT MANY OF THE TAF SITES. HOWEVER...DRIER AIR BELOW 3K FEET WILL SLOWLY BE ADVANCING IN FROM THE NORTH WHICH HAS ALREADY ADVECTED IN AT MBS. THIS WILL LEAD TO A SLOW BUT STEADY INCREASE IN CEILING HEIGHTS FROM NORTH TO SOUTH DURING THE COURSE OF THE MORNING AND AFTERNOON. THIS WILL OCCUR DESPITE THE INCREASING COVERAGE OF RAINFALL. A STRONG NORTHEASTERLY PRESSURE GRADIENT WILL CONTINUE TO LEAD TO GUSTY WINDS...ESPECIALLY AT MBS WHERE FUNNELING DOWN SAGINAW BAY IS LEADING TO SOME LOCALLY STRONGER WINDS UP TO 40 KNOTS. THE RAIN SHOULD END AT ALL OF THE TAF SITES DURING THE EVENING HOURS WITH VFR CONDITIONS EXPECTED AS LOW PRESSURE PUSHES EAST TOWARDS THE ATLANTIC SEABOARD.

&&

.PREV DISCUSSION...ISSUED 332 AM EDT SUN MAY 15 2011

SHORT TERM...TODAY

A LOW PRESSURE SYSTEM OVER THE EASTERN OHIO VALLEY WILL BEGIN ITS

TRACK EASTWARD TOWARDS THE ATLANTIC SEABOARD TODAY. BEFORE IT MOVES OFF TO THE EAST SHOWERS ARE EXPECTED TO CONTINUE ACROSS MUCH OF THE AREA TODAY UNDER AN 850-500MB DEFORMATION ZONE ON THE COLD SIDE OF THIS LOW. DRY AIR IN PLACE ACROSS THE NORTHERN GREAT LAKES WILL BEGIN TO SINK SOUTHWARD AS THE LOW DEPARTS...SLOWLY SHUTTING OFF THE SHOWERS FROM NORTH TO SOUTH. WHILE THE SOUTHERN CWA WILL REMAIN VERY MOIST WITH CONTINUED SHOWER ACTIVITY ALL OF TODAY...THE SAGINAW VALLEY AND NORTHERN THUMB SHOULD SEE AN END TO THE RAIN BY THE AFTERNOON HOURS AS THIS DRY AIR ADVECTS IN. THE VERY TIGHT PRESSURE GRADIENT ON THE NORTH SIDE OF THIS LOW HAS CREATED VERY GUSTY WINDS ACROSS LAKE HURON EARLY THIS MORNING. THESE WINDS HAVE FUNNELED DOWN SAGINAW BAY AND CHANNLED THESE STRONG WINDS INTO THE SAGINAW VALLEY WITH WIND GUSTS REACHING 50 MPH AT TIMES. WITH THIS FLOW EXPECTED TO LAST FOR MUCH OF TODAY HAVE ISSUED A WIND ADVISORY FOR BAY AND MIDLAND COUNTIES WITH FREQUENT GUSTS OF 40 TO 50 MPH EXPECTED MUCH OF TODAY. WINDS WILL DIE DOWN LATER THIS AFTERNOON AS THE LOW DEPARTS AND WINDS SHIFT TO THE NORTH WITH A LOOSER PRESSURE GRADIENT. WILL TAKE THE ADVISORY THROUGH 4 PM AND CANCEL EARLIER IF WINDS DROP BELOW ADVISORY CRITERIA SOONER. WITH THE REGION ON THE COLD SIDE OF THE LOW PRESSURE SYSTEM AND CLOUDY RAINY CONDITIONS EXPECTED FOR MUCH OF THE DAY WITH MIXING HEIGHTS ONLY TO 925MB THE DIURNAL TEMPERATURE RANGE SHOULD NOT BE VERY LARGE AS HIGHS WILL ONLY BE A FEW DEGREES WARMER THAN MORNING LOWS.

LONG TERM...

COOL AND BRISK START TO THE WORK WEEK. EXPANSIVE UPPER LEVEL RIDGE AND SURFACE HIGH PRESSURE OVER CENTRAL CANADA WILL DRIFT TO THE SOUTH OVER THE NEXT 48 HOURS AND ENOUGH DRY AIR IS EXPECTED TO FILTER INTO SOUTHEAST MICHIGAN TO ALLOW FOR A DRY MONDAY...AS WEAKENING 500 MB LOW LIFTS NORTH FROM THE EASTERN OHIO VALLEY. SHOWERS WILL LIKELY BE CLOSE BY HOWEVER...ALONG THE US/CANADIAN BORDER. 850 MB TEMPS NOW PROGGED TO FALL SLIGHTLY BELOW ZERO DURING MONDAY...SETTING UP A COLD NIGHT MONDAY NIGHT...IN ADDITION TO TONIGHT. IT APPEARS PRESSURE GRADIENT WILL BE TOO STRONG TO ALLOW WINDS TO DECOUPLE (ESPECIALLY WITH NORTHEAST FLOW OFF LAKE HURON)...AND ALTHOUGH WE ARE LIKELY LOOKING AT MINS IN THE MID 30S ACROSS A PORTION OF SOUTHEAST MICHIGAN...NOT PLANNING ON MENTIONING ANY FROST WITH THE WIND STAYING UP. PLUS...THIS IS NO GUARANTEE CLOUDS ARE GOING TO FULLY CLEAR OUT TONIGHT...AND CLOUDS WILL LIKELY BE RETURNING FOR MONDAY NIGHT. LATEST TRENDS FOR THE SHEARED OUT ENERGY OVER THE DAKOTAS/IOWA IS TO DIVE SOUTHEAST...MUCH FARTHER SOUTH...WITH THE CENTER OF THIS SHORTWAVE HOVERING AROUND FAR EASTERN TENNESSEE OR EVEN NORTHERN GEORGIA MONDAY/TUESDAY. NONE-THE-LESS...THE

LARGE SCALE UPPER LEVEL LOW/TROUGH IS QUITE EXTENSIVE...AND GOOD TAP OF ATLANTIC MOISTURE IS STILL PROGGED TO ADVANCE WESTWARD INTO THE CENTRAL GREAT LAKES ON TUESDAY...WITH LEAD SURGE OF LOW LEVEL WARM ADVECTION...AS 850 MB TEMPS FORECASTED TO CLIMB INTO THE MID SINGLE NUMBERS. BETTER UPPER LEVEL FORCING AS WE HEAD INTO THE MID WEEK PERIOD...AS THE MID/UPPER LEVEL CIRCULATION ADVANCES NORTH INTO THE WESTERN MID ATLANTIC STATES. THE GOOD NEWS IS AN UPPER LEVEL RIDGE IS FORECASTED (PER 00Z GFS/EUROPEAN) TO BUILD INTO THE GREAT LAKES REGION AS WE HEAD INTO THE WEEKEND...SUPPORTING A QUICK WARM UP...WITH TEMPERATURES POTENTIALLY BACK TO 80 DEGREES BY SATURDAY. \$\$ MARINE... THE PRESSURE GRADIENT WILL CONTINUE TO TIGHTEN AS LOW PRESSURE LIFTS THROUGH THE OHIO VALLEY TO WESTERN PENNSYLVANIA BY MORNING AND HIGH PRESSURE SHIFTS SLOWLY SOUTHEAST TOWARDS THE REGION. THIS SETUP WILL PROVIDE A PROLONGED PERIOD OF NORTHEASTERLY FLOW...WHICH WILL PEAK EARLY THIS MORNING...BUT PERSIST TO SOME DEGREE INTO EARLY NEXT WEEK AS THIS LOW PRESSURE SYSTEM STALLS NEAR THE APPALACHIAN RANGE. NORTHEAST WINDS ARE STILL GUSTING TO GALE FORCE DUE TO THE FUNNELING EFFECT UP SAGINAW BAY AND EXPECT WINDS SPEEDS TO REMAIN AT THESE LEVELS THROUGH THE AFTERNOON HOURS...THEREFORE WILL RETAIN THE GALE WARNING THROUGH ITS CURRENT EXPIRATION. WILL ALSO MAINTAIN THE SMALL CRAFT ADVISORIES FOR THE REMAINDER OF THE LAKE HURON NEAR SHORE WATERS AS WIND SPEEDS SHOULD GENERALLY PEAK CLOSER TO 30 KNOTS WITHOUT THE HELP OF FUNNELING. FOR THE SAME REASON...WILL CONTINUE TO FORGO A GALE WARNING FOR THE OPEN WATERS AS WINDS GENERALLY REMAIN IN THE LOWER 30 KNOT RANGE. WILL KEEP THE SMALL CRAFT ADVISORIES FOR LAKE ST CLAIR AND FAR WESTERN LAKE ERIE TODAY AS STRONGER NORTHEAST FLOW PENETRATES INTO THESE AREAS AS THE AFOREMENTIONED LOW PRESSURE MOVES EAST OF THE CENTRAL LAKES REGION. WITH THIS LONG PERIOD OF NORTHEAST/NORTH WINDS...WAVES WILL BUILD TO 10 FEET OR MORE OVER PORTIONS OF LAKE HURON TONIGHT INTO SUNDAY AND THEN REMAIN HIGH FOR SEVERAL DAYS THEREAFTER && .DTX WATCHES/WARNINGS/ADVISORIES... MI...WIND ADVISORY...MIZ048-MIZ053...UNTIL 4 PM SUNDAY. LAKE HURON... GALE WARNING...SAGINAW BAY AND THE NEARSHORE WATERS FROM PORT AUSTIN TO HARBOR BEACH...UNTIL 4 PM SUNDAY. SMALL CRAFT ADVISORY...NEARSHORE WATERS FROM HARBOR BEACH TO PORT HURON...UNTIL 8 AM MONDAY. LAKE ST CLAIR... SMALL CRAFT ADVISORY...UNTIL 10 PM SUNDAY. MI WATERS OF LAKE ERIE...SMALL CRAFT ADVISORY...UNTIL 10 PM SUNDAY. && \$\$ AVIATION.....KURIMSKI SHORT TERM...KURIMSKI LONG TERM....SF MARINE.....KURIMSKI YOU CAN OBTAIN YOUR LATEST NATIONAL WEATHER SERVICE FORECASTS ONLINE AT WWW.WEATHER.GOV/DETROIT (ALL LOWER CASE).

2.2 Sample nr2a, nr2b

540
FXUS63 KDTX 032319
AFDDTX

AREA FORECAST DISCUSSION
NATIONAL WEATHER SERVICE DETROIT/PONTIAC MI
719 PM EDT SUN JUL 3 2011

.AVIATION...

//DISCUSSION...

JUST EXPECT A FEW SHOWERS TO DOT THE AREA FROM DET/DTW SOUTH AS LAKE BREEZES INTERACT AND HELP RELEASE MINOR LOW LEVEL INSTABILITY FROM DAYTIME HEATING TODAY. OTHERWISE...VFR CONDITIONS ARE EXPECTED WITH LIGHT WINDS AS HIGH PRESSURE REMAINS IN PLACE OVER FROM THE CENTRAL GREAT LAKES TO UPPER MIDWEST.

FOR DTW...MAY SEE AN ISOLATED SHOWER OR TWO EARLY IN THE FORECAST PERIOD AS LAKE BREEZE INTERACTIONS CONTINUE TO PRODUCE LOCALLY ENHANCE LOW LEVEL CONVERGENCE OVER THE REGION.

//DTW THRESHOLD THREATS...

* LOW CONFIDENCE OF CEILINGS AROUND 5000 FEET EARLY IN THE FORECAST FROM ISOLATED SHOWERS.

&&

.PREV DISCUSSION...ISSUED 336 PM EDT SUN JUL 3 2011

SHORT TERM...TONIGHT

MUCH NICER DAY TODAY WITH HIGHS SOLIDLY IN THE 80S ALONG WITH LOWER HUMIDITY. 24 HR CHANGE IN TEMP/DEW PT AVERAGING 10 DEGREES LOWER.

AGITATED BUT DISORGANIZED AND HIGH BASED CU FIELD OVER THE SOUTH HALF OF THIS AFTERNOON AND CANT TOTALLY RULE OUT ISOLATED SHOWER/THUNDERSTORM OVER THE NEXT COUPLE OF HOURS WITH MLCAPES OF 400 TO 800 J/KG...BUT WITH MEAGER SURFACE/LOW LEVEL CONVERGENCE AROUND AND SURFACE DEW PTS EXPECTED TO DROP WITH FURTHER MIXING/ADVECTION PROCESSES...WILL LEAVE THE MENTION OUT. SKIES WILL THEN TREND TO MOSTLY CLEAR/CLEAR OVERNIGHT AS HIGH

PRESSURE CONTINUES TO WORK ITS WAY IN FROM THE WEST. FAVORABLE RADIATING NIGHT SHOULD ALLOW FOR A GOOD PORTION OF THE CWA TO SNEAK INTO THE 50S...WITH WARMER URBAN AREAS IN THE LOWER 60S.

LONG TERM...MONDAY THROUGH NEXT SUNDAY

HIGH PRESSURE WILL BE IN CONTROL OF THE WEATHER FOR THE 4TH OF JULY HOLIDAY. THE HIGH WILL PROVIDE MOSTLY CLEAR SKIES AND LIGHT WINDS AS HIGH TEMPERATURES CLIMB INTO THE 80S. THIS HIGH PRESSURE SYSTEM WILL SLOWLY SINK SOUTH MONDAY NIGHT...AS A LOW PRESSURE SYSTEM TRACKS THROUGH THE GREAT LAKES REGION TUESDAY AND WEDNESDAY. ALTHOUGH RAIN IS NOT EXPECTED ON TUESDAY...THE EFFECTS OF THE APPROACHING LOW WILL STILL BE APPARENT WITH WARMER TEMPERATURES AS WINDS TURN TO THE SOUTHWEST AND INCREASING CLOUDS FROM THE APPROACHING COLD FRONT FROM THE NORTH.

THE FRONT ITSELF IS A RATHER WEAK FEATURE...HOWEVER THE SHORTWAVE COINCIDENT WITH THE FRONT WILL BE THE MAIN DRIVING FORCE BEHIND THE SHOWER AND THUNDERSTORM ACTIVITY TUESDAY NIGHT AND WEDNESDAY. CURRENT MODEL RUNS ARE IN FAIRLY GOOD AGREEMENT ON THE TIMING OF THE ACTIVITY...WITH VERY LITTLE ADJUSTMENT FROM THE PREVIOUS FORECAST. THE BEST CHANCE FOR RAIN WILL BE ON WEDNESDAY AS THE SHORTWAVE TAKES ADVANTAGE OF MLCAPE VALUES AROUND 1 J/G. DESPITE THE CAPE VALUES...THE WIND FIELD IS EXPECTED TO BE RATHER WEAK WITH NOT MUCH SHEAR TO SPEAK OF AND FREEZING LEVELS ARE FORECAST TO BE AROUND 13K FT SO SEVERE WEATHER DOES NOT LOOK TO BE A BIG ISSUE AT THIS POINT.

THE MODEL DATA CONTINUES TO LINGER A WEAKER SHORTWAVE ACROSS THE EXTREME SOUTHEASTERN CWA WEDNESDAY EVENING...WARRANTING THE CONTINUATION OF POPS DURING THIS PERIOD. HOWEVER HIGH PRESSURE WILL QUICKLY BUILD IN BEHIND THE DEPARTING FRONT LATER WEDNESDAY NIGHT...PROVIDING DRY AND SLIGHTLY COOLER WEATHER ON THURSDAY.

A SURFACE HIGH OF 1019MB WILL BE CENTERED OVER THE GREAT LAKES FOR FRIDAY AND SATURDAY LEADING TO DRY WEATHER AND TEMPERATURES VERY CLOSE TO THE CLIMO NORMS. NWP GUIDANCE IS MOSTLY WITHIN 3 DEGREES...SO WENT WITH AN OVERALL BLEND OF MOS GUIDANCE. MID RUN GFS DOES SHOW A WEAK SHORTWAVE MOVING THROUGH MICHIGAN ON SATURDAY THAT COULD SPARK SOME CONVECTIVE SHOWERS...BUT 12Z HAS SINCE SQUASHED THAT NOTION AND WILL PROBABLY JUST GET BY WITH SOME AFTERNOON CU.

MARINE...

TRANQUIL CONDITIONS WILL PERSIST ACROSS AREA WATERS FOR THE REMAINDER OF THE HOLIDAY WEEKEND WITH WINDS EXPECTED TO RANGE FROM 5 TO 10 KNOTS FOR MOST AREAS THROUGH AT LEAST WEDNESDAY WHEN THE A FRONT WILL BRING A BRIEF INCREASE IN WINDS AND THE NEXT CHANCE FOR THUNDERSTORMS LATE TUESDAY INTO WEDNESDAY.

&&

.DTX WATCHES/WARNINGS/ADVISORIES...

MI...NONE.

LAKE HURON...NONE.

LAKE ST CLAIR...NONE.

MI WATERS OF LAKE ERIE...NONE.

AVIATION.....DG

SHORT TERM...SF

LONG TERM....KURIMSKI/MM

MARINE.....SF

2.3 Sample nr6

043

FXUS63 KDTX 290734

AFDDTX

AREA FORECAST DISCUSSION

NATIONAL WEATHER SERVICE DETROIT/PONTIAC MI

334 AM EDT FRI JUL 29 2011

.SHORT TERM...TODAY

AREAS OF CONVECTION CONTINUE TO FLARE UP ALONG A STALLED FRONTAL BOUNDARY STRETCHING ACROSS THE WESTERN AND CENTRAL GREAT LAKES THIS MORNING. THIS IS BEING ENHANCED BY A COMBINATION OF A MID-LEVEL MCV AND BY A NOCTURNAL LOW-LEVEL JET WHICH IS NOSING UP INTO MICHIGAN. NUMEROUS THUNDERSTORMS ARE EXPECTED SOUTH OF I-69 EARLY THIS MORNING...WITH ACTIVITY STRETCHING FROM SOUTHEAST MICHIGAN BACK TOWARDS THE CHICAGO AREA (THE LATTER OF WHICH WILL AFFECT SOUTHERN LOWER MICHIGAN LATER THIS MORNING). GOOD ELEVATED INSTABILITY LOOKS PRESENT ACROSS THIS AREA PER MODEL CROSS-SECTIONS AND FORECAST SOUNDINGS...POTENTIALLY SUPPORTING UPDRAFTS STRONG ENOUGH FOR STORMS TO BECOME SEVERE. OTHER BIG CONCERN IS THE POTENTIAL FOR

FLASH FLOODING AS STRONGER STORMS MAY PRODUCE RAINFALL RATES BETWEEN 1 AND 2 INCHES PER HOUR. MUCH OF THIS RAIN WILL FALL OVER GROUND THAT REMAINS SATURATED FROM RAIN LAST NIGHT.

COLD FRONT WILL DROP ACROSS LOWER MICHIGAN LATER THIS MORNING AS A MID-LEVEL TROUGH PUSHES ACROSS ONTARIO. THIS WILL PUSH SHOWERS AND THUNDERSTORMS OUT OF THE AREA BY LATE AFTERNOON AND ALLOW DEWPOINTS TO FALL SLIGHTLY. THIS FRONT WILL HOWEVER DO LITTLE TO COOL TEMPERATURES.

&&

.LONG TERM...FRIDAY NIGHT THROUGH NEXT WEEK

THE LOW TO MID LEVEL FLOW IS FORECAST TO BE MORE NORTHWESTERLY BY TONIGHT IN THE WAKE OF THE DEPARTING MID LEVEL SHORT WAVE. THIS WILL HELP ADVECT THE MUCH DRIER AIRMASS NOW OBSERVED OVER NORTHERN MINNESOTA INTO SOUTHERN MICHIGAN DURING THE COURSE OF THE NIGHT...ENDING THE RISK FOR ANY ADDITIONAL RAINFALL. WEAK HIGH PRESSURE AND MUCH DRIER AIR WILL BECOME ESTABLISHED OVER SE MI BY SATURDAY...WHICH WILL LEAD TO SUNNY SKIES WITH MORE COMFORTABLE HUMIDITY LEVELS. DESPITE SOME WEAK LOW LEVEL COLD AIR ADVECTION TONIGHT...MODEL SOUNDINGS SUGGEST AMPLE DAYTIME INSOLATION WILL SUPPORT DEEP MIXING HEIGHTS SAT AFTERNOON. THIS SUPPORTS LEANING TOWARD THE HIGH END OF GUIDANCE MAX TEMPS...UPPER 80S TO NEAR 90 WITH SOME MARINE MODIFICATION KEEPING THE THUMB REGION A TOUCH COOLER.

THE ELONGATED UPPER RIDGE NOW OVER THE SOUTHERN US IS FORECAST TO RETROGRADE BACK INTO THE SOUTH-CENTRAL PLAINS DURING THE COURSE OF THE WEEKEND...WHILE A FAIRLY DEEP MID LEVEL TROUGH SLIDES INTO EASTERN CANADA. THIS WILL LEAD TO SUBSTANTIAL HEIGHT FALLS ACROSS EASTERN CANADA AND NRN NEW ENGLAND BY EARLY NEXT WEEK. ASSOCIATED WITH THIS TROUGH WILL BE A SURFACE FRONT...FORECAST TO DROP INTO SOUTHERN MICHIGAN LATE SUN INTO SUN NIGHT. THERE WILL BE A NARROW RIBBON OF DEEP LAYER MOISTURE ALONG THIS FRONT. INSTABILITY IS FORECAST TO BE SOMEWHAT MARGINAL AT THIS POINT. THE 00Z MODEL SUITE DO HOWEVER SHOW SOME EXIT REGION JET SUPPORT AND FAIRLY DIFFLUENT FLOW ALOFT...WHICH SUPPORTS THE A CHANCE OF CONVECTION LATE SUNDAY THROUGH SUNDAY NIGHT.

THE MEDIUM RANGE SOLUTIONS ALL INDICATE A STRENGTHENING MID LEVEL RIDGE OVER THE SOUTHERN/CENTRAL PLAINS NEXT WEEK...WHICH HAS BEEN THE DOMINATE PATTERN OVER MUCH OF THE SUMMER. THERE WILL BE THE POTENTIAL FOR CONVECTIVE SYSTEM ORIGINATING OVER THE

NRN PLAINS/UPPER MIDWEST TO SLIDE INTO LOWER MI UNDER THE NORTHWEST FLOW. TIMING AND PROBABILITY OF THESE SYSTEMS IS QUITE LOW THIS FAR OUT. THE CURRENT FORECAST HAS THE NEXT CHANCE OF THUNDERSTORMS ON TUES...WHICH IS IN LINE WITH THE RECENT MODEL CONSENSUS. DEPENDING ON TIMING OF ANY CONVECTIVE COMPLEXES...TEMPS ARE EXPECTED TO REMAIN ABOVE SEASONAL NORMS WITH THE GREAT LAKES REGION BEING ON THE FRINGE OF THE STRONG SUBTROPICAL RIDGE.

&&

.MARINE...

SHOWER AND THUNDERSTORM ACTIVITY SHOULD DIMINISH BY MID-AFTERNOON AS A WEAK COLD FRONT DROPS THROUGH THE AREA. HIGH PRESSURE BUILDING INTO THE REGION WILL PROVIDE DRY WEATHER AND LIGHT WINDS FROM THIS EVENING INTO SUNDAY. A COLD FRONT WILL THEN DROP THROUGH THE AREA AS LOW PRESSURE TRACKS ACROSS HUDSON BAY. THIS WILL BRING CHANCES FOR SHOWERS AND THUNDERSTORMS LATE SUNDAY AND SUNDAY NIGHT. WESTERLY WINDS ASSOCIATED WITH THE FRONTAL PASSAGE ARE EXPECTED TO REMAIN BELOW 15 KNOTS.

&&

.AVIATION...ISSUED 1252 AM EDT FRI JUL 29 2011

//DISCUSSION...

A CONVECTIVE COMPLEX WILL CONTINUE TO EVOLVE DURING THE EARLY MORNING HOURS IMPACTING THE FLINT AND PONTIAC TERMINALS MOST DIRECTLY. TRENDS LOOK PRETTY SOLID WITH THE STRONGEST ACTIVITY CONFINED NEAR THE INTERSTATE 69 CORRIDOR EARLY IN THE OVERNIGHT WITH THE PATTERN THEN DEVELOPING TO THE SOUTH AND EAST TOWARD SUNRISE BEFORE EXITING THE AREA BY MID MORNING. FOG WILL TEND TO FORM IN THE TRAILING BOUNDARY LAYER MOISTURE WITH ANY LINGERING SHOWERS AND THUNDERSTORMS MINGLED WITH A PERIOD OF MVFR CEILING ASSOCIATED WITH PASSAGE OF THE SURFACE TROUGH/Front. STEADY IMPROVEMENT TO VFR BY AFTERNOON IS THEN EXPECTED AS WEAK HIGH PRESSURE BUILDS INTO THE REGION TOWARD EVENING.

FOR DTW...THUNDERSTORM ACTIVITY WILL TRACK NEARBY TO THE NORTH AND WEST OF THE AIRPORT FOR MUCH OF THE NIGHT BEFORE ACTIVITY TRAILING WESTWARD TOWARD CHICAGO MOVES INTO THE REGION. RELYING ON THE TRAILING ACTIVITY TENDS TO LOWER CONFIDENCE THAT THE AIRPORT WILL BE IMPACTED BUT TRENDS WILL BE MONITORED AND TIMING REFINED DURING THE EARLY MORNING HOURS. WHILE THERE IS

SOME UNCERTAINTY ON THUNDERSTORM IMPACTS, CONFIDENCE IS HIGHER ON CEILING TRENDS WITH LESS THAN 5000 FT EXPECTED WITH THE RAIN ALONG WITH A PERIOD OF MVFR CEILING ASSOCIATED WITH THE FRONTAL PASSAGE THROUGH MID MORNING. STEADY IMPROVEMENT BACK INTO VFR IS THEN EXPECTED FOR THIS AFTERNOON.

//DTW THRESHOLD THREATS...

* MODERATE CONFIDENCE THUNDERSTORMS WILL AFFECT DTW 08Z TO 11Z.

* HIGH CONFIDENCE CEILING BELOW 5000 FT DURING THE MORNING.

&&

.PREV DISCUSSION...ISSUED 1043 PM EDT THU JUL 28 2011

CONVECTIVE TRENDS HAVE SHOWN UP STRONGLY ENOUGH SINCE THE LAST UPDATE TO SUPPORT THE CONTINUATION OF THE FLASH FLOOD WATCH, EVEN FOR METRO DETROIT. THE MCV CROSSING NORTHERN LOWER MICHIGAN WILL CONTINUE TO SUPPORT BACKED FLOW OVER SOUTHERN LOWER MICHIGAN IN THE MIDST OF THE LOW LEVEL MOISTURE AXIS WITH PRECIPITABLE WATER IN THE RANGE OF 2 TO 2.5 INCHES ACCORDING TO HOURLY MESOANALYSIS.

IF ANYTHING, COVERAGE SHOULD INCREASE AS THE MCV SUPPORTS A RAMPED UP LOW LEVEL JET AND ACCELERATED MOISTURE TRANSPORT TO THE SOUTH OF ITS TRACK AND OVER SE MICHIGAN. THIS WILL FUEL CONVECTION STRONGLY ENOUGH FOR A FEW STORMS TO POSSIBLY APPROACH SEVERE LIMITS, AND THIS WILL BE MONITORED, BUT HEAVY RAINFALL CLEARLY REMAINS THE PRIMARY CONCERN THROUGH THE NIGHT. THE TRACK OF THE MCV AND THE POSITION OF THE LOW LEVEL THETA-E RIDGE STILL FAVOR THE SAGINAW VALLEY AND NORTHERN THUMB, AND THE NORTHERN PORTION OF THE WATCH AREA, FOR THE HEAVIEST RAINFALL BUT COVERAGE WILL BE GREAT ENOUGH TOWARD THE DETROIT AREA TO MAINTAIN THE HEADLINE.

&&

.DTX WATCHES/WARNINGS/ADVISORIES...

MI...FLASH FLOOD WATCH...MIZ053-MIZ060-MIZ061-MIZ062-MIZ063-MIZ068-MIZ069-MIZ070-MIZ075-MIZ076-MIZ082-MIZ083...UNTIL 11 AM FRIDAY.

LAKE HURON...NONE.

LAKE ST CLAIR...NONE.

MI WATERS OF LAKE ERIE...NONE.

&&

\$\$

SHORT TERM...HLO
LONG TERM....SC
MARINE.....HLO
AVIATION.....BT

YOU CAN OBTAIN YOUR LATEST NATIONAL WEATHER SERVICE FORECASTS
ONLINE
AT WWW.WEATHER.GOV/DETROIT (ALL LOWER CASE).

2.4 Sample nr12

433
FXUS63 KDTX 240510
AFDDTX

AREA FORECAST DISCUSSION
NATIONAL WEATHER SERVICE DETROIT/PONTIAC MI
110 AM EDT WED AUG 24 2011

.AVIATION...

//DISCUSSION...

SHOWERS WITH SOME EMBEDDED THUNDERSTORMS WILL PERSIST
THROUGH ROUGHLY DAYBREAK...ASSOCIATED WITH AN UPPER LEVEL LOW
PRESSURE SYSTEM WHICH WILL BE ROTATING ACROSS LOWER MI EARLY
THIS MORNING.

RECENT VAD WIND PROFILE DATA ALONG WITH 00Z MODEL SOUNDINGS
INDICATE STRENGTHENING WINDS ABOVE THE NOCTURNAL INVERSION THIS
MORNING...PROMPTING A MENTION OF LOW LEVEL WIND SHEAR THROUGH
13Z.

WITH THE EXPECTATION THAT AMPLE LOW LEVEL MOISTURE WILL BE IN
PLACE BELOW THIS INVERSION SHORTLY AFTER DAYBREAK...WILL
CONTINUE TO CARRY A BRIEF PERIOD OF MVFR BASED STRATUS LATER THIS
MORNING. THERE IS A CHANCE OF STRONG THUNDERSTORMS ALONG A COLD
FRONT FORECAST TO MOVE ACROSS THE REGION LATE THIS
AFTERNOON/EVENING.

FOR DTW...A LITTLE MORE ROBUST INSTABILITY IS NOW FORECAST TO MOVE

INTO METRO DETROIT IN THE 08Z TO 12Z TIME PERIOD...WHICH LOOKS TO GIVE DTW A GOOD SHOT AT SOME THUNDERSTORMS EARLY THIS MORNING. GUSTY SOUTH-SOUTHWEST WINDS WILL THEN DEVELOP BY AFTERNOON IN ADVANCE OF A COLD FRONT. WIND GUSTS MAY APPROACH OR EXCEED 30 KNOTS MID TO LATE WED AFTERNOON.

//DTW THRESHOLD THREATS...

* HIGH CONFIDENCE IN THUNDERSTORM CHANCES PRIOR TO 12Z.

* MEDIUM CONFIDENCE IN CLOUD BASES BELOW 5000 FT LATE THIS MORNING.

* HIGH CONFIDENCE SOUTHWEST WIND GUSTS WILL EXCEED 25 KNOTS THIS AFTERNOON.

* MEDIUM CONFIDENCE IN STRONG THUNDERSTORM DEVELOPMENT THIS EVENING.

&&

.PREV DISCUSSION...ISSUED 946 PM EDT TUE AUG 23 2011

UPDATE...

A CLUSTER OF SHOWERS AND SCATTERED THUNDERSTORMS HAVE DEVELOPED OVER SW LOWER MI OVER THE LAST COUPLE OF HOURS. THIS CONVECTION IS A RESULT OF WARM AIR ADVECTION ON THE NOSE OF STRENGTHENING LOW LEVEL INFLOW. THIS IS ALL IN ADVANCE OF A POTENT MID LEVEL TROUGH OVER NE WISCONSIN. THIS SYSTEM WILL INVOKE PRETTY DECENT MID LEVEL HEIGHT FALLS ACROSS LOWER MI TONIGHT AS IT TRACKS EAST. CONTINUED LOW-MID LEVEL THETA E ADVECTION IN THE PRESENCE OF THIS FORCING SHOULD ALLOW DECENT COVERAGE OF SHOWERS TO CONTINUE TO PUSH EAST INTO THE FORECAST AREA DURING THE REMAINDER OF THE NIGHT. THE 00ZDTX SOUNDING SHOWED NO INSTABILITY OVER SE MI...WHICH EXPLAINS WHY THE THUNDERSTORMS HAVE THUS FAR BEEN UNABLE TO MAKE THE TRIP INTO SE MI. MID LEVEL COOLING WILL HOWEVER STEEPEN THE LAPSE RATES DURING THE COURSE OF THE NIGHT...WHICH WILL ALLOW ENOUGH ELEVATED INSTABILITY TO POSE THE RISK OF SOME THUNDERSTORM DEVELOPMENT...ESPECIALLY LATE. OVERALL...THE GOING FORECAST LOOKS IN GOOD SHAPE. THUS AN UPDATE WILL BE ISSUED STRICTLY TO REMOVE THE TIMING OF SHOWERS AS THEY ARE VIRTUALLY ON THE DOORSTEP.

PREV DISCUSSION...ISSUED 400 PM EDT TUE AUG 23 2011

SHORT TERM... TONIGHT

A BATCH OF SHOWERS AND THUNDERSTORMS HAVE BEEN IMPACTING NORTHERN ILLINOIS THROUGH MUCH OF THE DAY...SLIGHTLY IMPACTING/DELAYING MOISTURE SURGE INTO LOWER MICHIGAN...AS SURFACE DEW PTS REMAIN IN THE COMFORTABLE MID 50S TO AROUND 60 RANGE ACROSS MOST OF SOUTHEAST MICHIGAN THROUGH 2 PM. HOWEVER...AS THUNDERSTORM COMPLEX CONTINUES TO HEAD SOUTH...SOME OF THAT DEEPER MOISTURE OVER THE MIDWEST (IOWA) WILL WORK INTO SOUTHERN LOWER MICHIGAN. MOISTURE TRANSPORT VECTORS/THETA-E FIELDS SHOW MID LEVEL MOISTURE (700 MB) ARRIVING AROUND 00Z...WITH LOW LEVEL MOISTURE (850 MB) AROUND 6Z. EXPECTATIONS ARE CONVECTION WILL RE-ORGANIZE OVER WISCONSIN LATER TODAY...CLOSE/UNDERNEATH THE MID LEVEL CIRCULATION. THIS MID LEVEL WAVE WILL BE BOOTED TO THE EAST TONIGHT...AS DYNAMIC...CLIPPER LIKE SYSTEM COMES OUT OF SOUTHERN SASKATCHEWAN. THE 850-700 MB THETA-E RIDGE AXIS LOOKS TO BE GETTING PINCHED OFF AS IT MOVES INTO OUR AREA...WITH CORRESPONDING INSTABILITY WEAKENING (SEE SHOWALTER INDICES). NONE-THE-LESS...WITH MID LEVEL CIRCULATION TRACKING OVER/CLOSE TO THE STRAIGHTS OVERNIGHT AND SUBSEQUENT MODEST HEIGHT FALLS EXTENDING SOUTH...ALONG WITH THE 850 THETA-E MOISTURE/CONVERGENCE...EXPECTING NUMEROUS SHOWERS AND EMBEDDED THUNDERSTORMS...JUST NOT AS CONCERNED WITH THE HEAVY RAIN DUE TO THE PROGRESSIVE NATURE AND LESS INSTABILITY. LEFT INHERITED MINS INTACT...MID 60S WITH THE WARM ADVECTION PATTERN AND HIGHER DEW PTS MOVING IN...IN LINE WITH LATEST MAV GUIDANCE. LONG TERM... WEDNESDAY THROUGH NEXT TUESDAY

THANKS TO THE ACCOMPANYING SHORT WAVE, NOCTURNAL CONVECTION AND ASSOCIATED CLOUD COVER WILL BE TO OUR EAST BY MID WEDNESDAY MORNING.

THIS WILL OPEN THE DOOR ON SURFACE HEATING FOR THE NEXT ROUND OF STORMS AS THE PREFRONTAL TROUGH/COLD FRONT MOVES THROUGH SE MICHIGAN. THERE IS SOME RESIDUAL BOUNDARY LAYER MOISTURE INDICATED THAT COULD TRANSLATE INTO SOME STRATUS FOR A WHILE BUT THIS APPEARS OVERDONE IN THE MODEL DATA BASED ON SATELLITE IMAGERY OVER THE MIDWEST DURING THE MORNING. SHOULD LOW CLOUD COVER BE ABLE TO MATERIALIZE, IT WILL MIX OUT QUICKLY AS SURFACE HEATING AND SOUTHWEST WINDS RAMP UP BY AFTERNOON. SEVERE WEATHER POTENTIAL AND TIMING THEN BECOME THE MAIN PROBLEM IN THE FORECAST FOR WEDNESDAY AFTERNOON AND EVENING.

THE BIG THING, WHICH WAS DOCUMENTED THOROUGHLY IN THE EARLY MORNING FORECAST PACKAGE, IS THE INCREASE IN THE MODEL WIND FIELD AND INSTABILITY PARAMETERS FOR WEDNESDAY AFTERNOON AND

EVENING. THIS HAS CARRIED OVER INTO THE 12Z FORECAST CYCLE ADDING CONFIDENCE TO THE POTENTIAL FOR SEVERE CONVECTION. THE LATEST FORECAST SOUNDINGS FROM THE NAM AND GFS SPORT 0-1KM MLCAPE OF 2000-2500 J/KG BY LATE AFTERNOON VS 1500 COMPARED TO YESTERDAYS DATA. THIS APPEARS TO BE THE RESULT OF A BETTER HANDLE ON THE EML MIGRATING INTO THE MIDWEST FROM THE PLAINS. THERE IS ALSO CONSIDERABLY GREATER SHEAR IN THE LOW LEVELS OF THE WIND PROFILE, DUE TO EXTRA DEEPENING OF THE SURFACE LOW IN NORTHERN ONTARIO, WITH 0-3KM HELICITY RANGING FROM 250-300 M2/S2 COMPARED TO VALUES CLOSER TO 150 YESTERDAY. THE DATA IN YESTERDAY'S MODEL RUNS DEPICTED A SCENARIO SUFFICIENT FOR SEVERE WEATHER, ESPECIALLY WITH REGARD TO LINEAR CONVECTIVE MODES, BUT THE NUMBERS THAT HAVE PERSISTED INTO TODAY'S MODEL DATA INTRODUCE AN EXTRA LAYER OF POTENTIAL THAT INCLUDES SUPERCCELL MODES CAPABLE OF LARGE HAIL AND TORNADO DEVELOPMENT. THE MOST CHALLENGING ASPECT OF THE FORECAST WILL BE IDENTIFYING THE TIMING AND LOCATION FOR STORM INITIATION. THIS IS COMPLICATED BY THE LOW TO MID LEVEL CAPPING INVERSION THAT DEVELOPS ON THE HEELS OF THE EARLY MORNING ACTIVITY AND STRENGTHENED BY THE INCREASING SOUTHWEST LOW LEVEL FLOW DURING THE EARLY AFTERNOON. AT THIS POINT, PREFER TO EXPECT THE CAP TO HOLD INTO THE LATE AFTERNOON/AROUND 21Z. AFTER THAT, SURFACE CONVERGENCE ALONG THE PREFRONTAL TROUGH WILL COMBINE WITH MAX TEMPS NEAR 90 AND THE APPROACH OF THE UPPER TROUGH TO INITIATE STORMS. BY THEN, HOWEVER, THE ACTIVITY WILL LIKELY DEVELOP RIGHT OVER SE MICHIGAN BEFORE MOVING OFF TO THE EAST BY MID EVENING. THIS WOULD RESULT IN VERY LITTLE ADJUSTMENT TO EARLIER EXPECTATIONS FOR SEVERE WEATHER OTHER THAN POSSIBLY SPARING US THE MORE MATURE ASPECTS OF SQUALL LINE DEVELOPMENT IN OUR AREA.

A BROAD EXPANSE OF HIGH PRESSURE WILL THEN SETTLE OVER THE GREAT LAKES FOR THE END OF THE WEEK. THIS WILL BRING COOLER AND LESS HUMID CONDITIONS BACK INTO SE MICHIGAN FOR THURSDAY AND FRIDAY. DRY CONDITIONS WILL BE PUNCTUATED BY LOW TEMPERATURES MAKING A RUN BACK DOWN INTO THE UPPER 40S IN THE TYPICALLY COOLER LOCATIONS IN OUR AREA. THE BROAD HIGH PRESSURE SYSTEM IS ALSO SHOWN TO CONTINUE GUARDING US AGAINST MUCH MOISTURE RETURN AHEAD OF THE NEXT COLD FRONT DUE BY SATURDAY AFTERNOON.

THE LARGE SCALE PATTERN IN THE WESTERLIES IS SHOWN IN THE LATEST GLOBAL MODELS TO PRESERVE SOME TROUGHINESS IN THE UPPER LEVEL PATTERN OVER EASTERN NORTH AMERICA BY THE BEGINNING OF NEXT WEEK.

THERE IS VERY LITTLE AMPLIFICATION UPSTREAM, HOWEVER, SO WE CONTINUE TO EXPECTED A SUPPLY OF SHORT WAVES FROM THE EASTERN PACIFIC AND WESTERN CANADA INTO THE GREAT LAKES. A FAIRLY LARGE

SHORT WAVE IS INDICATED IN THE GREAT LAKES AROUND MONDAY BUT WITH TIMING AND TRACK COMPLICATIONS EXPECTED BY THE PRESENCE OF "IRENE", EVEN THOUGH IT WILL REMAIN LARGELY TO OUR EAST THROUGH TUESDAY.

MARINE...

SOUTHWEST WINDS WILL BE RAMPING UP TONIGHT...BUT ESPECIALLY TOMORROW AHEAD OF A COLD FRONT...WITH FREQUENT GUSTS OF 20 TO 30 KNOTS EXPECTED ACROSS THE MARINE AREAS. A SMALL CRAFT ADVISORY HAS BEEN ISSUED FOR ALL NEARSHORE WATERS. SCATTERED THUNDERSTORMS ARE EXPECTED TO BE AROUND TONIGHT AS WARM FRONT MOVES THROUGH. THESE STORMS ARE NOT EXPECTED TO BE SEVERE. OF MORE CONCERN ARE THE THUNDERSTORMS WHICH DEVELOP ALONG THE COLD FRONT LATE TOMORROW...WHICH WILL HAVE THE POTENTIAL TO PRODUCE WINDS OF 50 KNOTS OR GREATER. WINDS BEHIND THE COLD FRONT WILL SHIFT TO THE NORTHWEST...AND WILL REMAIN STRONG OVER THE NORTH HALF OF THE LAKE HURON WEDNESDAY NIGHT INTO THURSDAY. WINDS WILL DIMINISH ON FRIDAY AS HIGH PRESSURE RETURNS.

&&

.DTX WATCHES/WARNINGS/ADVISORIES...
MI...NONE.

LAKE HURON...

SMALL CRAFT ADVISORY...NEARSHORE WATERS FROM PORT AUSTIN TO PORT HURON INCLUDING SAGINAW BAY...FROM 8 AM WEDNESDAY TO 8 PM WEDNESDAY.

LAKE ST CLAIR...

SMALL CRAFT ADVISORY...FROM 8 AM WEDNESDAY TO 8 PM WEDNESDAY.

MI WATERS OF LAKE ERIE...

SMALL CRAFT ADVISORY...FROM 8 AM WEDNESDAY TO 8 PM WEDNESDAY.

&&

\$\$

AVIATION.....SC
UPDATE.....SC
SHORT TERM...SF
LONG TERM....BT
MARINE.....SF

YOU CAN OBTAIN YOUR LATEST NATIONAL WEATHER SERVICE FORECASTS
ONLINE AT WWW.WEATHER.GOV/DETROIT (ALL LOWER CASE).

Supplementary Text 3: Diffusive mass transfer of noble gases in a raindrop and calculation of average raindrop sizes from measured noble gases in rainwater

1. Introduction

Overall mass-dependent noble gas patterns for rainwater samples from southeast Michigan display simultaneous atmospheric He excesses and Ne, Ar, Kr and Xe depletion with respect to ASW (Fig. 1c, main text). As mentioned in section 5 of the manuscript, these patterns cannot originate from liquid rainwater that equilibrated at higher altitudes. Instead, they can be accounted for if precipitation originates as ice (cf. Section 5, Fig. 2, main text). Multiple lines of weather evidence, including observations of hail (direct observation of hail was observed for samples nr10-1 and 13 while weather data indicate hail for samples nr4-1,4-2,5-2,6,9,10-2,12 and 13; see Text S1, Table S2) during sample collection as well as examination of probable condensation altitudes (cf. Text S1) suggest that precipitation originating as ice is likely in southeast Michigan. Below, in section 2, we first describe a simple mass-transfer model involving diffusion in a sphere (raindrop), which is used to qualitatively show that noble gas patterns in Michigan rainwater samples originate from ice (Fig. 2, section 5, main text). Subsequently, in section 3 below, we use this diffusion model and a more rigorous quantitative approach, to evaluate the time-dependent evolution of noble gas patterns in raindrops assuming a constant equilibrium boundary condition and noble gas diffusion coefficients. In section 4 below, the time-dependent evolution of noble gas patterns in raindrops is discussed in the context of varying equilibrium boundary conditions and noble gas diffusion coefficients used in the model. The effects of boundary conditions and diffusion coefficients assumed in sections 2-4 on the rate of noble gas incorporation into a raindrop are compared in section 5. Finally, in section 6, a novel application of dissolved noble gases in rainwater is demonstrated. Specifically, a procedure for estimating average raindrop sizes using the diffusion model together with measured rainwater noble gas concentrations is outlined.

2. Diffusive Mass-Transfer in Raindrop Model Description and Calculation of Isothermal Equilibrium Stages of Noble Gases in a Raindrop

Diffusion of noble gases into a raindrop can be simulated using a simple mass-transfer model in a sphere. The total amount of noble gases diffusing into or out of a sphere with a constant concentration at the surface is given by the infinite series solution [*Crank, 1975*]:

$$F_i = 1 - \frac{6}{\pi^2} \sum_{n=1}^{\infty} \frac{1}{n^2} \exp(-n^2 \pi^2 X) \quad (1)$$

or,

$$F_i = 6X^{0.5} \left\{ \pi^{-0.5} + 2 \sum_{n=1}^{\infty} \operatorname{ierfc} \frac{n}{\sqrt{X}} \right\} - 3X \quad , \text{ if } X < 0.182873063 \quad (2)$$

where F_i is the fraction of noble gas 'i' (where, 'i'=He, Ne, Ar, Kr and Xe) transferred at any given time 't', parameter $X=Dt/a^2$, where 'a' is the radius of raindrop, 'D' is the diffusion coefficient of noble gases and 'n' is the nth term of the infinite series solution. Equations (1) and (2) provide the basis to calculate diffusive mass transfer in a raindrop of a particular size.

If one assumes that: a) noble gas concentrations in raindrops start as ice (see section 5 of main text) and; b) noble gas concentrations of ice crystals within clouds are similar to the average ice concentrations in Lake Vida, Antarctica [see section 5 of main text, *Malone et al.*, 2010], expected noble gas patterns as mass transfer proceeds within a raindrop starting from ice and reaching different stages of isothermal equilibrium ($F_i=1$; assuming ASW at 0°C) can be calculated (Fig. 2, main text) by:

$$F_i = \frac{\left(\frac{C_m}{C_{eq}} - \frac{C_{ice}}{C_{eq}} \right)}{\left(1 - \frac{C_{ice}}{C_{eq}} \right)} \quad (3)$$

or, Equation (3) may also be written as:

$$C_m = F_i \times (C_{eq} - C_{ice}) + C_{ice} \quad (4)$$

where F_i is the fraction of noble gas ‘i’ as defined earlier (equations 1, 2), C_m , C_{eq} , C_{ice} are the measured, equilibrium and average ice noble gas concentrations. Using equation (3), model expected noble gas patterns (C_m/C_{eq} ; green dotted lines, Fig.2, main text) can be calculated for various stages of equilibration (F_i values between 0-100%) using initial average ice concentrations, C_{ice}/C_{eq} equal to 1.383, 0.825, 0.097, 0.064 for He, Ne, Ar, Kr and Xe (solid green line, Fig.2, main text; *Malone et al.*, 2010). For example, to derive the expected noble gas patterns for 50% equilibration (green dotted lines, Fig.2, main text), C_{ice}/C_{eq} values from *Malone et al.* [2010] is used for each noble gas with $F_i=0.5$ in equation (3) to calculate (C_m/C_{eq}). This yields model values (C_m/C_{eq}) of 1.192, 0.913, 0.549, 0.532 and 0.525 for He, Ne, Ar, Kr and Xe respectively and is plotted as the 50% equilibration line (green dotted lines, Fig.2, main text). Model expected noble gas patterns are similarly derived for various stages of equilibration assuming initial average ice concentrations from *Malone et al.* [2010] and F_i values between 0-100%. It is important to note here that model noble gas patterns derived in Figure 2 (main text) is time-independent and represents a simple, qualitative analysis of the evolution of noble gas patterns from ice to equilibrium values. Actual noble gas concentrations within a raindrop are expected to evolve at different rates as discussed in section 3 of this supplementary text.

Such a qualitative comparison of model-expected and measured noble gas patterns (cf. Fig.2, main text) suggests that this simple model is capable of reproducing atmospheric He excesses together with Ne, Ar, Kr and Xe depletion patterns observed in our Michigan rainwater samples when they are assumed to evolve from ice. For example, sample nr4-2 indicates measured He and Ne concentrations within 50%-60% of equilibrium with the atmosphere while Ar, Kr and Xe point to equilibration values between 60% and 70% (Fig. 2, main text). Ar, Kr and Xe point to greater equilibration values than He and Ne due to increased dissolution of the heavier noble gases in rainwater resulting from heat transfer, a process which is not accounted for in our simple diffusive mass-transfer model. Indeed, evaporation of a falling raindrop lowers the droplet’s surface temperature compared to its surroundings leading to greater dissolution of the more temperature sensitive heavier noble gases Ar, Kr and Xe [see, e.g., *Elperin et al.*, 2007]. A comprehensive treatment of transient, coupled heat and mass transfer of noble gases within a falling raindrop is out of the scope of the present manuscript. However, our simple diffusion mass transfer model qualitatively shows that mass-dependent noble gas patterns are expected in rainwater if the latter is assumed to start as ice. To further support our conclusion, we use a more rigorous

quantitative approach and evaluate the time-dependent evolution of noble gases within a raindrop as described below.

3. Time-dependent evolution of noble gas patterns within a raindrop assuming a constant equilibrium boundary condition and noble gas diffusion coefficients

The time-dependent evolution of noble gas patterns within a falling raindrop is simulated using the diffusive mass transfer model for a sphere discussed earlier (equations 1-3, supplementary text 3) in addition to the following assumptions: a) noble gas concentrations in raindrops start as ice (see section 5 of the main text) and; b) noble gas concentrations of ice crystals within clouds are similar to the average ice concentrations in Lake Vida, Antarctica [Malone *et al.*, 2010]. Expected noble gas patterns (C_m/C_{eq}) within a raindrop starting from ice can be determined at any given time 't' by first calculating parameter 'F_i', which is the fraction of noble gas 'i' (where, 'i'=He, Ne, Ar, Kr and Xe) transferred at any given time 't' using equations (1) and (2). Subsequently, using equation (3) and initial average ice concentrations, C_{ice}/C_{eq} equal to 1.383, 0.825, 0.097, 0.064 for He, Ne, Ar, Kr and Xe (solid green line, Fig. S9a; Malone *et al.*, 2010) model expected noble gas patterns (C_m/C_{eq}) for any time 't' may be derived (blue, red lines, Fig. S9a).

For example, Figure S9a shows the evolution of noble gas patterns within a raindrop starting from ice (green markers, Fig.S9a) and reaching isothermal equilibrium (=1; assuming ASW at 0°C) at various times 't' for a 5mm droplet derived using equations 1-3 (blue, red markers, Fig. S9a). However, equations 1 and 2 require knowledge of the diffusion coefficients of noble gases 'D'. Because the raindrop simulations represent a phase transition from solid ice to liquid water, model noble gas patterns are calculated using noble gas diffusion coefficients in both liquid water (blue markers, Fig.S9a) and solid ice (red markers, Fig.S9a). Liquid water noble gas diffusivities were assumed at a temperature of ~0°C because diffusion in liquid water is slowest at 0°C and this will yield maximum time to equilibration. However, because noble gas diffusion coefficients in liquid water are only well known between 5 and 35°C [Jähne *et al.*, 1987], values at 0°C were approximated by the following temperature dependency [Eyring, 1936]:

$$D_i = A_i \times \exp(E_a/RT) \quad (5)$$

where D_i is the diffusion coefficient for noble gas 'i' (where i=He, Ne, Ar, Kr, Xe) at any temperature 'T' (°K), 'R' is the universal gas constant of 8.314 J/K-mol, 'E_a' and 'A' are fit parameters for each noble gas given by Jähne *et al.* [1987]. Noble gas diffusivities in solid ice were calculated by mass-scaling the diffusion coefficient of CO₂ in ice from Antarctica ($D_{CO_2} = 7.24 \times 10^{-11} \text{ m}^2 \text{ s}^{-1}$ at -25.4°C; Ahn *et al.*, 2008) as follows:

$$D_{ice} = D_{CO_2} \times \left(\frac{M_{CO_2}}{M_i} \right)^{1/2} \quad (6)$$

where D_{ice} is the diffusion coefficient for noble gas 'i' (where i=He, Ne, Ar, Kr, Xe) in ice and M_{CO_2} and M_i are the mass of CO₂ and respective noble gas 'i'. Noble gas diffusion coefficients thus calculated in liquid water are ~1 or more orders of magnitude faster than in solid ice and are likely to represent extreme values (Table S3). Because of large variations in noble gas diffusion coefficients, the evolution of rainwater noble gas patterns are calculated at various times 't' for both diffusivity values in ice (red markers, Fig.S9a; t=200s, 1000s, 5000s, 50000s) and liquid water (blue markers, Fig. S9a; t=200s, 500s, 1000s, 5000s) using equations 1-3.

Figure S9a compares model-expected (red, blue markers) evolution of noble gas patterns in a raindrop with measured rainwater noble gas pattern for sample nr4-2 (black triangles). Such a comparison confirms results from our qualitative analysis (section 2, text S3) and indicates that mass-dependent noble gas patterns are expected in rainwater if the latter is assumed to start as ice. Specifically, this comparison shows that measured He and Ne concentrations for nr4-2 fall within the domain of model rainwater patterns for $t=1000s$ assuming diffusion coefficients in liquid water and ice (shaded region, Fig. S9a) while measured Ar, Kr and Xe concentrations for nr4-2 are marginally greater than model-prediction for $t=1000s$ assuming diffusivity of liquid water (blue marker dashed line, Fig. S9a) by 6%, 11% and 16%, respectively. As previously mentioned in section 2, the diffusive model under-predicts measured Ar, Kr and Xe concentrations due to increased dissolution of the temperature-sensitive heavy noble gases in rainwater resulting from cooling of droplet surface by evaporation of a falling raindrop, a process which is not accounted for in our simple diffusive mass-transfer model. In addition, Fig.S9 also shows that the evolution of rainwater noble gas patterns is faster when noble gas diffusivity values in liquid water (blue marker, Fig.S9a) are assumed as compared to ice (red marker, Fig.S9a). Nevertheless, irrespective of the absolute time taken, rigorous calculation of time-dependent evolution of noble gas patterns in rainwater confirms that mass-dependent rainwater noble gas patterns originate from ice.

For the sake of simplicity, the diffusive model calculations used so far assumed a constant equilibrium boundary condition with noble gas composition in raindrops going from ice to ASW at $0^{\circ}C$ (sections 2, 3). However, in reality, raindrops experience variations in temperature and pressure as they fall through the atmosphere. In the next section, we discuss the time dependent evolution of rainwater noble gas patterns assuming variable equilibrium boundary conditions and diffusion coefficients in the context of varying temperature and pressure experienced by a falling raindrop.

4. Time-dependent evolution of noble gas patterns in a raindrop assuming variable equilibrium concentrations and diffusion coefficients

In sections 2 and 3 of this supplementary text, the evolution of noble gas patterns within a raindrop was calculated using the simplifying assumption of a constant equilibrium boundary condition at the surface of a droplet (ASW at $0^{\circ}C$) as well as constant noble gas diffusion coefficients. However, in reality, raindrops experience variations in temperature and pressure (altitude) as they fall through the atmosphere. Because noble gas concentrations are dependent on temperature and altitude (partial pressure), equilibrium noble gas concentrations at the surface of a falling rain droplet will vary (red circles, Fig.2, main text). As previously mentioned in section 5 of main text, because of lower pressures at high altitude, equilibrium He and Ne concentrations are lower than ASW values at the ground surface as these gases are mostly sensitive to pressure (red circles, Fig.2, main text). In contrast, the heavier noble gases Ar, Kr and Xe are particularly sensitive to temperature and the impact of low temperatures at altitude dominates over that of low pressures leading to expected concentrations at higher altitudes higher than ground surface ASW values (red circles, Fig.2, main text). In addition, variations in temperature will also affect the noble gas diffusion coefficients (cf. equation 5, Text S3). Specifically, an increase in ambient

atmospheric temperature with decreasing altitude leads to faster noble gas diffusion coefficients (cf. equation 5, Text S3). Below, we investigate the time-dependent evolution of noble gas concentrations within a raindrop when equilibrium noble gas concentrations as well as noble gas diffusion coefficients are varying during droplet fall.

Because equilibrium noble gas concentrations and diffusion coefficients vary as a function of temperature and altitude, the evolution of noble gas patterns within a well-mixed falling raindrop is computed at discrete, multiple time steps using the diffusive mass transfer model for a sphere (equations 1-3, Text S3) together with assumptions on the noble gas composition of ice crystals within clouds discussed earlier (sections 2, 3, Text S3). At each time step 't' (time interval=0.01s), noble gas diffusion coefficients are first calculated based on the ambient temperature of the atmosphere at that altitude using equation (5). Calculated noble gas diffusion coefficients are used to determine parameter F_i , which is the fraction of noble gas 'i' (where, 'i'=He, Ne, Ar, Kr and Xe) transferred at any given time 't' using equations (1) and (2) that are derived for a constant boundary condition. A constant boundary condition approximation is valid here because within the small time interval modeled (t=0.01s corresponding to ~10m drop in altitude for a 5mm raindrop), large transient variations in equilibrium atmospheric noble gas concentrations are not expected. Subsequently, model expected noble gas patterns (C_m) for any time 't' is derived using equation (4) together with initial average ice concentrations (C_{ice} ; see sections 2, 3, Text S3) and equilibrium noble gas concentrations corresponding to a particular altitude and temperature (C_{eq}). This procedure is illustrated through a specific example below.

Figure S9b compares measured noble gas concentrations of sample nr4-2 together with the time-dependent evolution of noble gas patterns from ice for a 5mm droplet assuming variable equilibrium concentrations and diffusion coefficients. The raindrop is assumed to fall from an altitude of ~4500m through an atmosphere with a temperature lapse rate of 6.072°C/km. Likely altitude of condensation (~4500m) and lapse rate were determined from sounding data (cf. Text S1) as well as from the measured surface temperature for nr4-2 at the time of collection (26°C; Table S1). Fig. S9b shows the effect of varying temperature and altitude on equilibrium noble gas concentrations (C_{eq} ; red markers). Model expected noble gas patterns (C_m) are calculated using the procedure outlined above for every second. Figure S9b shows the evolution of noble gas patterns within the raindrop from ice at 50s, 100s, 200s, 300s, 400s and 443s, at which point the raindrop reaches the ground based on our assumptions of droplet size and condensation altitude. Comparison of model evolution of noble gas patterns in a raindrop (green dotted markers, Fig. S9b) with measured rainwater noble gas pattern for sample nr4-2 (black triangles) confirms our previous results from section 2 and 3 of this supplementary text and indicates that mass-dependent noble gas patterns are expected in rainwater if the latter is assumed to start as ice. Indeed, Fig. S9b shows that measured He and Ne concentrations for nr4-2 compare well with model rainwater patterns ($C_{model}-C_{meas}<5\%$) while measured Ar, Kr and Xe concentrations for nr4-2 are marginally greater than model-prediction for t=443s by 9%, 11% and 15%, respectively. As previously mentioned in sections 2 and 3 the diffusive model under-predicts measured Ar, Kr and Xe concentrations due to increased dissolution of the heavier noble gases in rainwater resulting from surface cooling during evaporation of a falling droplet, a process which is not accounted for in our simple diffusive mass-transfer model. Results of evolution of noble gas concentrations within a raindrop obtained using variable equilibrium noble gas concentrations and diffusion coefficients are similar to the results obtained by using a

constant equilibrium boundary condition (sections 2, 3, Text S3). Thus, irrespective of the boundary condition used, our calculations show that mass-dependent rainwater noble gas patterns clearly originate from ice. These results are in agreement with multiple lines of weather evidence, including direct observations of hail for samples nr10-1 and 13, weather data during sample collection which indicate hail for samples nr4-1,4-2,5-2,6,9,10-2,12 and 13 (see Text S1, Table S2) as well as examination of probable condensation altitudes (cf. Text S1) that suggest precipitation originating as ice is likely in southeast Michigan.

5. Comparison of the effects of boundary conditions and noble gas diffusion coefficients assumed on the rate of noble gas incorporation into a raindrop

While all the different boundary conditions and noble gas diffusion coefficients investigated in sections 2-4 clearly point to an ice origin of mass-dependent rainwater noble gas patterns, the different assumptions yield varying rates of noble gas incorporation into a raindrop. Figure S10 compares the time evolution of individual noble gases within a raindrop of size 5mm based on the assumed boundary conditions and diffusion coefficients used in sections 2-4. If a constant equilibrium boundary condition is used (sections 2 and 3), equilibration of all noble gases within the raindrop is faster assuming diffusion coefficients for liquid water (red line, Fig. S10) as compared to solid ice (green line, Fig. S10). This is because noble gas diffusion coefficients in liquid water are 1-2 orders of magnitude faster than in solid ice (cf. Table S3). However, when a variable equilibrium condition is used together with varying liquid water diffusion coefficients (section 4; blue line, Fig.S10), evolution of all noble gases except Ne is faster as compared to constant boundary condition (red line, Fig.S10). Such a pattern cannot only be due to the temperature-effect of noble gas diffusion coefficients because they tend to be faster at higher temperatures and lower altitudes for all noble gases (cf. equation 5). Instead, faster equilibration of all noble gases except Ne is observed when a variable equilibrium condition is used because model expected noble gas values (C_m) at any time 't' is dependent on the term ($C_{eq} - C_{ice}$) as shown in equation (4). For all noble gases except Ne, the term ($C_{eq} - C_{ice}$) is greater when a variable equilibrium condition is used (red circles, green triangles, Fig.S9b) as compared to constant equilibrium condition (solid black line, green triangles, Fig. S9b). By contrast, ($C_{eq} - C_{ice}$) for Ne is lower when a variable equilibrium condition is used (red circles, green triangles, Fig.S9b) as compared to constant equilibrium condition (solid black line, green triangles, Fig. S9b). This leads to a slightly slower equilibrium of rainwater noble gas patterns for Ne assuming a variable boundary condition as compared to a constant boundary condition.

However, irrespective of the boundary condition used, our calculations shown in sections 2-4 indicate that mass-dependent rainwater noble gas patterns clearly originate from ice and are in agreement with multiple lines of weather evidence observed for these samples. Because mass-dependent rainwater noble gas patterns originate from ice, we demonstrate a novel application of dissolved noble gases in rainwater in the next section. Specifically, we outline a procedure to estimate average raindrop sizes using the diffusion model described in section 2 together with measured rainwater noble gas concentrations.

6. Calculation of droplet size using measured noble gas concentrations in rainfall

In addition to calculating expected noble gas patterns for diffusive mass transfer of noble gases into a raindrop, the model described in section 2, can also be used to provide a range of droplet sizes for corresponding rainfall event using measured noble gas concentrations in rainwater. Similar to the assumptions in section 2, if it is assumed that: a) noble gas concentrations in raindrops start as ice and; b) noble gas concentrations of ice crystals within clouds are similar to the average ice concentrations in lake Vida, Antarctica [Malone *et al.*, 2010], the total amount of noble gases transferred (parameter F_i) can be calculated for each rainwater sample collected using equation (3). From the calculated F_i value for a given sample (equation 3), parameter X is then calculated from the inverse of F_i as follows:

$$F_i^{-1} = X = \frac{2}{\pi} \left(1 - \sqrt{1 - \left(\frac{\pi \times F_i}{3} \right)} \right) - \frac{F_i}{3} \quad \text{if } (F_i < 0.9) \quad (7)$$

or,

$$F_i^{-1} = X = \frac{-1}{\pi^2} \log \left(\frac{\pi^2 (1 - F_i)}{6} \right) \quad \text{if } (F_i > 0.9) \quad (8)$$

Because $X = Dt/a^2$, the time taken ‘ t ’ by a specific noble gas in a raindrop of size ‘ a ’ to achieve the corresponding ‘ F_i ’ value can be calculated. Since the size of raindrop ‘ a ’ is unknown, the time required for equilibration F_i value to be achieved (parameter ‘ t ’ in equations 1 and 2) for a specific sample is calculated for a range of droplet diameters between 0.019 and 10mm (red lines, Fig. 3 main text) assuming liquid water diffusion coefficients for all noble gases at a temperature of 0°C (Table S3). This will yield the maximum possible equilibration times for each gas since diffusion is slowest at 0°C. The range of equilibration times (parameter ‘ t ’ in equations 1, 2) calculated from measured noble gas concentrations using the above procedure for each sample (red lines, Fig. 3 main text) is further compared with the time ‘ t_z ’ taken for a raindrop of specific size to fall to the ground from the cloud base (blue lines, Fig. 3 main text). ‘ t_z ’ is calculated as the ratio of cloud condensation altitude and the terminal velocity ‘ V_t ’ of a droplet, which is defined as the maximum velocity of a falling raindrop at which the gravitational force equals the drag force acting on the drop [see e.g., *Testik and Barros, 2007*]. Cloud condensation altitudes between 0.5 and 5 kms (Fig. 3 main text) were assumed based on most probable condensation altitudes from weather sounding data (Fig. S7) and terminal velocity was calculated using the formulations given by *Beard [1976]* for droplet diameters between 0.019 and 7mm (Fig. S11). Terminal velocities calculated using *Beard [1976]* formulations agree well with values obtained from empirical relations provided by *Rogers [1989]*, *Atlas et al. [1973]* and *Best [1950]* for droplet sizes between 0.08 and 1.5mm, 0.6 and 5.8mm and 0.3 and 6mm respectively (Fig. S11). Comparison of the time ‘ t ’ taken by a specific noble gas in a raindrop of size ‘ a ’ to achieve the corresponding ‘ F_i ’ value (red lines, Fig. 3 main text) calculated earlier and the time ‘ t_z ’ taken for a raindrop of specific size to reach the ground (blue lines, Fig. 3 main text), will yield a solution space of droplet size and equilibration time corresponding to any specific event. From weather sounding data (e.g., Fig. S7), if a specific condensation altitude can be identified (Table S4), the range of droplet sizes can further be constrained. This model approach is described further below with a specific example.

For example, sample nr4-2 shown in Figure 3 of the manuscript yields F_i values of 0.5, 0.5, 0.7, 0.7, 0.6 for He, Ne, Ar, Kr and Xe based on equation (3) and measured concentrations in rainwater and assuming an ice origin of noble gases in rainwater as

described above. Using equation (7), these F_i values yield X values of 0.038, 0.028, 0.078, 0.059 and 0.058 for He, Ne, Ar, Kr and Xe, respectively. Assuming raindrop diameters between 0.019 and 10mm, a range of time 't', taken to achieve the calculated X values is obtained and plotted in Fig 3 (red lines). The time 't' taken to achieve a certain value of X and consequently, F_i is faster for the lighter noble gases (He, Ne) as compared to the heavier noble gases (Ar, Kr, Xe). This can also be illustrated by the temporal evolution of noble gases in raindrops of 0.1mm and 5mm in radius at a given temperature (assumed as 0°C here; Fig. S12). As shown in Fig. S12, the lighter noble gases He and Ne reach equilibrium faster than Ar, Kr and Xe because of their higher diffusion coefficients for a given temperature as compared to the heavier noble gases (Table S3). The time 't' taken to achieve a certain value of X (red lines, Fig. 3 main text) is then compared with the time 't_z' for a raindrop to reach the ground (blue lines, Fig. 3 main text). Comparison of these two time values yields the area indicated as "solution space" (shaded area, Fig.3, main text) defined by equilibration times of 100, 300, 500, 1000s and droplet sizes of 0.38, 1.3 and 6.5mm diameter. However, this range of drop sizes can be further constrained using weather sounding data for this sample which indicates a likely condensation altitude of ~4.5km (15000 ft; at ~0°C; Table S4). Assuming this condensation altitude yields corresponding range of drop sizes between ~1 and ~6mm for the rainfall event during the nr4-2 sample collection (Fig. 3, main text). Similarly, average raindrop sizes can thus be estimated for different samples with mass-dependent patterns. Table S4 summarizes the range of raindrop sizes estimated for all mass-dependent samples (Fig. 1.c, main text) where weather-sounding data yields an approximate condensation altitude. Estimated drop sizes for mass-dependent samples are large and range between 0.45 and 10mm in diameter. These estimated droplet sizes generally fall within the maximum critical diameter of raindrops observed in nature, which, depending on the amount of airstream turbulence, is usually between 6-8mm but may reach diameters as large as 10mm [Rogers and Yau, 1989]. In addition, large drop sizes are generally associated with heavier rainfall (e.g., Marshall and Palmer [1948]). Because large drop sizes are estimated using our calculations above for samples with mass-dependent noble gas patterns, our results imply that precipitation events for these samples are associated with heavier rainfall. Indeed, heavy rainfall was observed both by direct observations and through surface weather station records during the collection of mass-dependent samples (Text S1).

Another interesting observation from these calculations is that small raindrops (fog) of 0.1mm or less in diameter would only take 0.39s, 0.78s, 1.27s, 2.09s, 2.76s or less to reach ~90% equilibrium for He, Ne, Ar, Kr and Xe (cf. Fig. S12). This suggests that, if only mass-dependent diffusive processes were occurring in fogs, concentrations of noble gases would be expected to be in equilibrium with the surface conditions. However, our measurements show that this is clearly not the case suggesting that additional processes that are not presently understood are affecting noble gases dissolution in fogs. Further detailed investigation, including analysis of noble gases in fogs is critical to understanding these processes. Such information is useful in the fields of meteorology, atmospheric and climate sciences, in addition to hydrology and environmental engineering.

References

- Ahn, J., M. Headly, M. Wahlen, E. J. Brook, P. A. Mayewski, and K. C. Taylor (2008), CO₂ diffusion in polar ice: observations from naturally formed CO₂ spikes in the Siple Dome (Antarctica) ice core, *Journal of Glaciology*, 54(187), 685-695.
- Atlas, D., R. C. Srivastava, and R. S. Sekhon (1973), Doppler radar characteristics of precipitation at vertical incidence, *Rev. Geophys.*, 11, 1-35.
- Beard, K. V. (1976), Terminal velocity and shape of cloud and precipitation drops aloft, *J. Atmos. Sci.*, 33, 851-864
- Best, A. C. (1950), Empirical formulae for the terminal velocity of water drops falling through the atmosphere, *Q. J. R. Meteorol. Soc.*, 76, 302-311.
- Crank, J. (1975), *The mathematics of diffusion*, viii, 414 p. pp., Clarendon Press, Oxford, [Eng].
- Elperin, T., A. Fominykh, and B. Krasovitev (2007), Evaporation and Condensation of Large Droplets in the Presence of Inert Admixtures Containing Soluble Gas, *Journal of the Atmospheric Sciences*, 64(3), 983-995.
- Eyring H. (1936) Plasticity and diffusion as examples of absolute reaction rates. *J. Chem. Phys.* 4, 283-291.
- Jähne B., Heinz G., and Dietrich W. (1987) Measurement of the diffusion coefficients of sparingly soluble gases in water. *J. Geophys. Res.* 92, C10., 10767-10776.
- Malone, J. L., M. C. Castro, C. M. Hall, P. T. Doran, F. Kenig, and C. P. McKay (2010), New insights into the origin and evolution of Lake Vida, McMurdo Dry Valleys, Antarctica - A noble gas study in ice and brines, *Earth and Planetary Science Letters*, 289(1-2), 112-122.
- Marshall, J. S., and W. M. Palmer (1948), The distribution of raindrops with size, *J. Meteorol.*, 5, 165-166.
- Rogers, R. R. (1989), Raindrop collision rates, *J. Atmos. Sci.*, 46, 2469-2472.
- Rogers, R. R., and M. K. Yau (1989), *A short course in cloud physics*, xiv, 290 p. pp., Butterworth-Heinemann, Oxford ; Boston.
- Testik, F. Y., and A. P. Barros (2007), Toward elucidating the microstructure of warm rainfall: A survey, *Rev. Geophys.*, 45(2), RG2003.

Supplementary Text 4: Time taken for noble gas disequilibrium patterns in rainfall to re-equilibrate at the surface

1. Introduction

Measured He, Ne, Ar, Kr and Xe concentrations in all rainwater samples from southeast Michigan are not in equilibrium with surface conditions and deviate from expected ASW values. Specifically, rainwater samples display a maximum deviation of 29%, -11%, -26%, -33% and -36% with respect to ASW for He, Ne, Ar, Kr and Xe, respectively (cf. Section 4, main text). Rainwater is typically assumed to re-equilibrate at surface conditions on the order of a few minutes [see e.g., *Mazor*, 1972; *Klump et al.*, 2007]. While *Mazor* [1972] did not provide any calculations for this assumption, *Klump et al.* [2007] utilize a simple calculation based on diffusive length of noble gases to show that a water film of several millimeters in thickness would be in equilibrium with the atmosphere within 10 min. However, neither study used actual rainwater measurements to calculate the time taken by noble gases in rainwater to re-equilibrate at the surface. Below, we utilize a detailed model of diffusion in a plane sheet of water to calculate the time required for our measured maximum disequilibrium patterns in rainwater to re-equilibrate at surface conditions using realistic water depth values from precipitation data in Michigan.

2. Model Description

The total amount of noble gases diffusing into or out of a plane sheet of water is given by the infinite series solutions [*Crank*, 1975]:

$$F_i = 1 - \sum_{n=0}^{\infty} \frac{8}{(2n+1)^2 \pi^2} \exp\left\{-\frac{(2n+1)^2 \pi^2 X}{4}\right\} \quad (1)$$

or,

$$F_i = 2(X)^{0.5} \left\{ \pi^{-0.5} + 2 \sum_{n=1}^{\infty} (-1)^n \operatorname{ierfc}\left(\frac{n}{\sqrt{X}}\right) \right\} \quad \text{if } X < 0.6465 \quad (2)$$

$$\text{where, } X = \frac{Dt}{l^2} \quad (3)$$

F_i is the fraction of noble gas 'i' (where, 'i'=He, Ne, Ar, Kr and Xe) transferred at any given time 't', 'l' is the depth of water (or thickness of water film), D is the diffusion coefficient of noble gases and 'n' is the nth term of the infinite series solution. Equations (1), (2) and (3) can be utilized to solve for parameter 'X' by setting $F_i=29\%$, -11% , -26% , -33% and -36% for He, Ne, Ar, Kr and Xe, respectively. From calculated values of 'X', the time 't' taken to re-equilibrate can be obtained from equation (3) given the diffusion coefficient 'D' of noble gases and water depth or thickness of water film 'l'. Diffusion coefficients at a temperature of 25°C were used in our calculations because it is close to the mean measured surface air temperature at the time of collection of rainwater samples (Table S1). Values for noble gas diffusion coefficients at 25°C are given by *Bourg and Sposito* [2008]. In addition, water depth or thickness of water film 'l' was chosen based on measured hourly precipitation data

from the Ann Arbor weather station during the period of sample collection (May-September, 2011). During the period of sample collection, precipitation as high as 8.2cms was recorded in one hour. While this represents an extreme value, multiple rainfall events record precipitation of 1cm or more in one hour during this time period. Consequently, we utilize a water depth of 1cm to calculate the time 't' required for noble gases in rainwater to re-equilibrate using equation (3). Results of these calculations are presented below.

3. Model Results and Discussion

Considering a water depth of 1 cm, the maximum measured He excess of 29% in rainfall would take 900.5s (or ~15 minutes) at 25°C to reach equilibrium with surface conditions. Similarly, maximum deviations of -11%, -26%, -33% and -36% for Ne, Ar, Kr and Xe measured in rainfall would take ~3.3mins, ~34mins, ~72mins and ~108mins, respectively, to reach equilibrium with surface conditions for a water depth of 1 cm and 25°C. Our calculations show that re-equilibration is faster for the lighter noble gases He and Ne as compared to the heavier noble gases Ar, Kr and Xe due to both their higher diffusion coefficients and lower initial disequilibrium levels with respect to surface conditions. In addition, it should be noted that a smaller water depth 'l' would also lead to shorter re-equilibration times for all noble gases, in addition to processes such as turbulent mixing, if present. Nevertheless, our calculations show that the typical assumption that re-equilibration of rainwater at the surface is completed within a few minutes [see e.g., *Mazor, 1972; Klump et al., 2007*] is more applicable for lighter noble gases and smaller water depths (<1cms) while heavier noble gases and greater water depths require re-equilibration times on the order of hours.

Noble gas concentrations of rainfall and fog will thus be recorded in groundwater systems if the time taken to re-equilibrate with surface conditions is greater than the time taken to reach the water table. This is likely the case at high altitudes of the Galapagos Islands where rapid water infiltration due to the presence of fractures or thin soil cover [*Warrier et al., 2012*] allows little time for noble gas to re-equilibrate at the surface. However, sedimentary aquifer systems typically have thicker unsaturated zones and longer infiltration times allowing sufficient time for rainwater to re-equilibrate with ground air. This, in turn, allows the use of noble gases in paleoclimate reconstructions (e.g. *Kipfer et al., 2002, Castro et al., 2007, 2012, Alvarado et al., 2009*).

References

- Ahn, J., M. Headly, M. Wahlen, E. J. Brook, P. A. Mayewski, and K. C. Taylor (2008), CO₂ diffusion in polar ice: observations from naturally formed CO₂ spikes in the Siple Dome (Antarctica) ice core, *Journal of Glaciology*, 54(187), 685-695.
- Alvarado, J. A. C., F. Barbécot, R. Purtschert, M. Gillon, W. Aeschbach-Hertig, and R. Kipfer (2009), European climate variations over the past half-millennium reconstructed from groundwater, *Geophysical Research Letters*, 36.
- Atlas, D., R. C. Srivastava, and R. S. Sekhon (1973), Doppler radar characteristics of precipitation at vertical incidence, *Rev. Geophys.*, 11, 1–35.
- Beard, K. V. (1976), Terminal velocity and shape of cloud and precipitation drops aloft, *J. Atmos. Sci.*, 33, 851–864
- Bernstein, B. C., Wolff, C. A., & McDonough, F. (2007). An Inferred Climatology of Icing Conditions Aloft, Including Supercooled Large Drops. Part I: Canada and the Continental United States. *Journal of Applied Meteorology and Climatology*, 46(11), 1857–1878.
- Best, A. C. (1950), Empirical formulae for the terminal velocity of water drops falling through the atmosphere, *Q. J. R. Meteorol. Soc.*, 76, 302–311.
- Bourg, I. C., and G. Sposito (2008), Isotopic fractionation of noble gases by diffusion in liquid water: Molecular dynamics simulations and hydrologic applications, *Geochimica et Cosmochimica Acta*, 72(9), 2237-2247.
- Castro, M. C., C. M. Hall, D. Patriarche, P. Goblet, and B. R. Ellis (2007), A new noble gas paleoclimate record in Texas—Basic assumptions revisited, *Earth Planet. Sci. Lett.*, 257, 170–187
- Castro, M. C., R. B. Warrier, C. M. Hall, and K. C. Lohmann (2012), A late Pleistocene-Mid-Holocene noble gas and stable isotope climate and subglacial record in southern Michigan, *Geophys. Res. Lett.*, 39(19), L19709.
- Crank, J. (1975), *The mathematics of diffusion*, viii, 414 p. pp., Clarendon Press, Oxford, [Eng].
- Elperin, T., A. Fominykh, and B. Krasovitev (2007), Evaporation and Condensation of Large Droplets in the Presence of Inert Admixtures Containing Soluble Gas, *Journal of the Atmospheric Sciences*, 64(3), 983-995.
- Eyring H. (1936) Plasticity and diffusion as examples of absolute reaction rates. *J. Chem. Phys.* 4, 283–291.
- Hall, C. M., M. C. Castro, K. C. Lohmann, and T. Sun (2012), Testing the noble gas paleothermometer with a yearlong study of groundwater noble gases in an instrumented monitoring well, *Water Resour. Res.*, 48(4), W04517.
- Jähne B., Heinz G., and Dietrich W. (1987) Measurement of the diffusion coefficients of sparingly soluble gases in water. *J. Geophys. Res.* 92, C10., 10767–10776.
- Kipfer, R., W. Aeschbach-Hertig, F. Peeters, and M. Stute (2002), Noble Gases in Lakes and Ground Waters, *Reviews in Mineralogy and Geochemistry*, 47(1), 615-700.
- Klump, S., Y. Tomonaga, P. Kienzler, W. Kinzelbach, T. Baumann, D. M. Imboden, and R. Kipfer (2007), Field experiments yield new insights into gas exchange and excess air formation in natural porous media, *Geochimica et Cosmochimica Acta*, 71(6), 1385-1397.
- Lippmann, J., M. Stute, T. Torgersen, D. P. Moser, J. A. Hall, L. Lin, M. Borcsik, R. E. S.

- Bellamy, and T. C. Onstott (2003), Dating ultra-deep mine waters with noble gases and ^{36}Cl , Witwatersrand Basin, South Africa, *Geochimica et Cosmochimica Acta*, 67(23), 4597-4619.
- Malone, J. L., M. C. Castro, C. M. Hall, P. T. Doran, F. Kenig, and C. P. McKay (2010), New insights into the origin and evolution of Lake Vida, McMurdo Dry Valleys, Antarctica - A noble gas study in ice and brines, *Earth and Planetary Science Letters*, 289(1-2), 112-122.
- Marshall, J. S., and W. M. Palmer (1948), The distribution of raindrops with size, *J. Meteorol.*, 5, 165-166.
- Mazor, E. (1972), Paleotemperatures and other hydrological parameters deduced from noble gases dissolved in groundwaters; Jordan Rift Valley, Israel, *Geochimica et Cosmochimica Acta*, 36(12), 1321-1336.
- Rogers, R. R. (1989), Raindrop collision rates, *J. Atmos. Sci.*, 46, 2469-2472.
- Rogers, R. R., and M. K. Yau (1989), *A short course in cloud physics*, xiv, 290 p. pp., Butterworth-Heinemann, Oxford ; Boston.
- Testik, F. Y., and A. P. Barros (2007), Toward elucidating the microstructure of warm rainfall: A survey, *Rev. Geophys.*, 45(2), RG2003.
- Warrier, R. B., M. C. Castro, and C. M. Hall (2012), Recharge and source-water insights from the Galapagos Islands using noble gases and stable isotopes, *Water Resour. Res.*, 48(3), W03508.

Table S1. Rainwater sampling location, date and time of collection, measured surface air temperature (T), noble gas concentrations and measured He isotopic ratios (R) normalized to atmospheric He ratio (R_a). Samples from Milan and Ann Arbor were collected at altitudes of 215m and 290m a.s.l respectively. Surface weather station records used to derive appropriate precipitation characteristics for corresponding rainfall event is also indicated.

Sample	Location	Date	Time	T	He	Ne	Ar	Kr	Xe	R/R _a ^b	+/- 1s	Surface weather station record used
			(UTC ^a)	(°C)	(x 10 ⁻⁸) (ccSTPg ⁻¹)	(x10 ⁻⁷) (ccSTPg ⁻¹)	(x 10 ⁻⁴) (ccSTPg ⁻¹)	(x 10 ⁻⁸) (ccSTPg ⁻¹)	(x 10 ⁻⁹) (ccSTPg ⁻¹)			
nr1	Milan	15/5/11	15:40	8.2	4.67	1.78	3.66	8.70	12.43	0.95	0.02	Ann Arbor
n2a	Milan	4/7/11	0:27	25.0	5.56	1.94	3.03	6.50	8.34	0.97	0.02	-
nr2b	Milan	4/7/11	0:27	25.0	4.57	1.67	2.57	5.20	6.48	0.93	0.02	-
nr3-1 ^c	Milan	23/7/11	15:00	27.0	4.67	1.55	2.13	4.21	4.87	-	-	Custer
nr3-2 ^c	Milan	23/7/11	15:30	21.4	4.63	1.74	2.63	5.29	6.55	0.98	0.03	"
nr4-1 ^c	Ann Arbor	23/7/11	21:35	26.0	4.62	1.70	2.69	5.28	6.42	0.98	0.03	Ann Arbor
nr4-2 ^c	Ann Arbor	23/7/11	21:35	26.0	4.99	1.55	1.99	3.91	5.10	0.93	0.03	"
nr5-1 ^c	Milan	27/7/11	23:40	23.5	4.51	1.71	2.68	5.51	7.30	1.05	0.02	Ann Arbor
nr5-2 ^c	Milan	28/7/11	5:00	22.5	5.28	1.74	2.80	5.72	7.43	1.03	0.04	"
nr6	Milan	29/7/11	8:25	22.6	4.37	1.64	2.60	5.30	7.26	0.98	0.02	Ann Arbor
nr7	Milan	3/8/11	7:00	24.0	5.44	1.80	2.92	6.05	7.78	0.96	0.12	Ann Arbor
nr8	Milan	6/8/11	18:40	28.6	4.39	1.68	2.72	5.49	7.17	0.99	0.14	Custer
nr9	Milan	9/8/11	9:35	20.8	4.72	1.72	2.87	5.94	7.56	1.18	0.16	Ann Arbor
nr10-1 ^c	Milan	9/8/11	21:05	23.1	5.22	1.68	2.74	5.48	6.94	1.15	0.07	Willow Run
nr10-2 ^c	Milan	9/8/11	21:55	20.3	4.44	1.66	2.65	5.41	6.75	1.02	0.03	"
nr11	Milan	14/8/11	11:40	18.4	4.96	1.79	2.99	6.55	8.88	1.05	0.03	Ann Arbor
nr12	Milan	24/8/11	7:50	19.6	4.52	1.78	3.23	7.03	9.61	1.05	0.04	Custer
nr13	Milan	4/9/11	0:47	23.9	5.32	1.82	3.02	6.75	8.84	0.92	0.04	Ann Arbor
nr14	Milan	9/9/11	15:10	18.5	5.06	1.78	3.14	6.91	9.38	1.04	0.03	Ann Arbor

^a UTC is Coordinated Universal Time. UTC=Eastern Standard time+4 hours during daylight savings in USA.

^b R is the measured ³He/⁴He ratio and R_a is the atmospheric ³He/⁴He ratio of 1.384x10⁻⁶ [Clarke et al., 1976]

^c Except for nr5-1 and nr5-2, all other samples were collected on the same day and almost at the same time (±1 hour) indicating that they are likely from the same storm system

Table S2: Compiled hourly surface weather observations from individual weather station records. Because of the large size of this data file, the reader is referred to the excel file included in the supplementary material. Data description for each column in Table S2 including units, abbreviations and weather codes are provided in detail by NCDC (<http://hurricane.ncdc.noaa.gov/cdo/3505doc.txt>).

Table S3. Noble gas diffusion coefficients in liquid water and ice

Diffusion coefficient	He (m ² s ⁻¹)	Ne (m ² s ⁻¹)	Ar (m ² s ⁻¹)	Kr (m ² s ⁻¹)	Xe (m ² s ⁻¹)
<i>Liquid water at ~0°C^a</i>	4.74E-09	2.34E-09	1.44E-09	8.77E-10	6.64E-10
<i>Ice at -25.4°C^b</i>	2.40E-10	1.07E-10	7.59E-11	5.24E-11	4.20E-11

^aDiffusion coefficients for liquid water calculated from *Eyring* [1936] and *Jähne et al.* [1987] as described in supplementary text 3

^bDiffusion coefficients for ice calculated by mass-scaling the diffusion coefficient of CO₂ in ice from Antarctica (*Ahn et al.*, 2008) as described in supplementary text 3

Table S4: Estimated raindrop sizes for individual precipitation events/samples based on diffusive mass-transfer model.

Mass-dependent sample	Likely condensation		Droplet size (mm)	
	altitude (kms)		Minimum	Maximum
n2a ¹	-		-	-
nr2b ¹	-		-	-
nr3-1 ¹	-		-	-
nr3-2 ¹	-		-	-
nr4-1	4.5		0.45	2
nr4-2	4.5		1.2	6
nr5-1	4.5		0.7	1.8
nr5-2	4.5		0.7	10
nr6	4.5		0.7	3
nr7	4.5		0.5	10
nr9	3		0.6	3
nr10-1	4		0.7	8
nr10-2	4		0.9	3
nr11	3		0.55	3
nr13	3.5		0.5	10

¹Weather Sounding not available

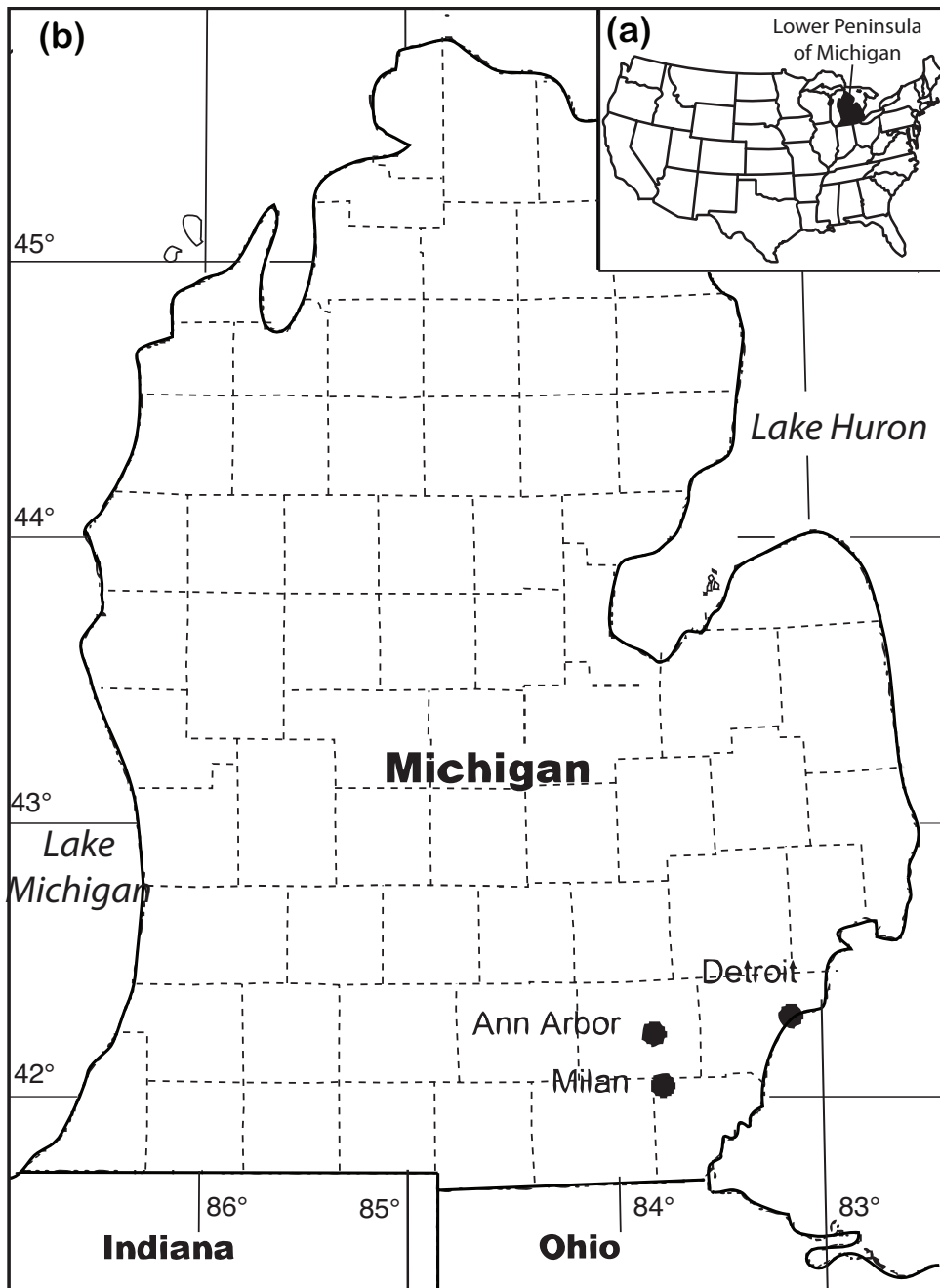


Figure S1: (a) Location of Michigan and (b) rainwater sample collection sites in Ann Arbor and Milan. Base map and locations are obtained through map services from U.S. Geological Survey, National Geospatial Program (<http://nationalmap.gov/>).

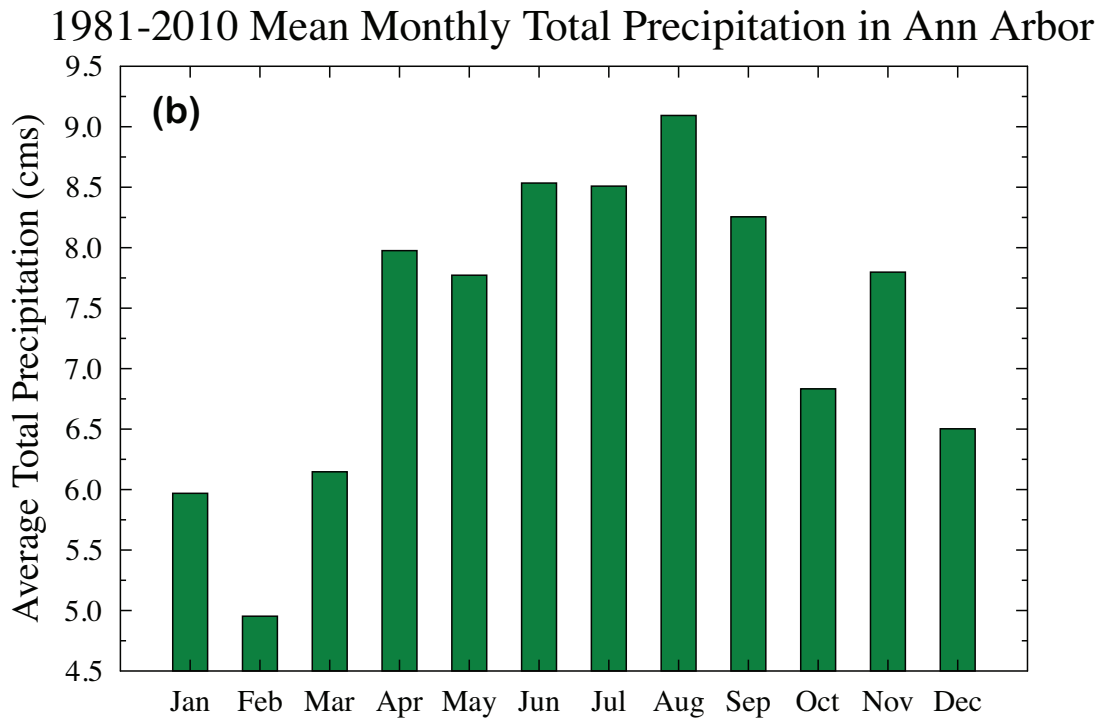
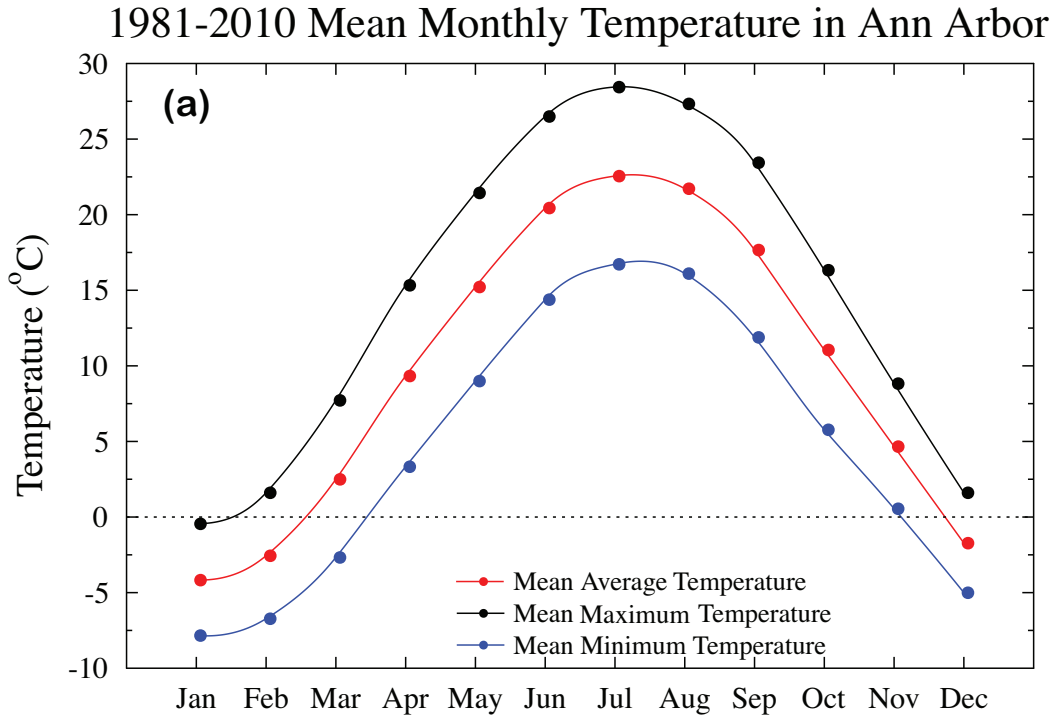


Figure S2: 1981-2010 Mean climatological summary for Ann Arbor (Station ID: USC00200230; 42.28°N, 83.77°W) located in southeast Michigan (a) Monthly mean total precipitation and (b) monthly mean maximum, minimum and average temperatures.

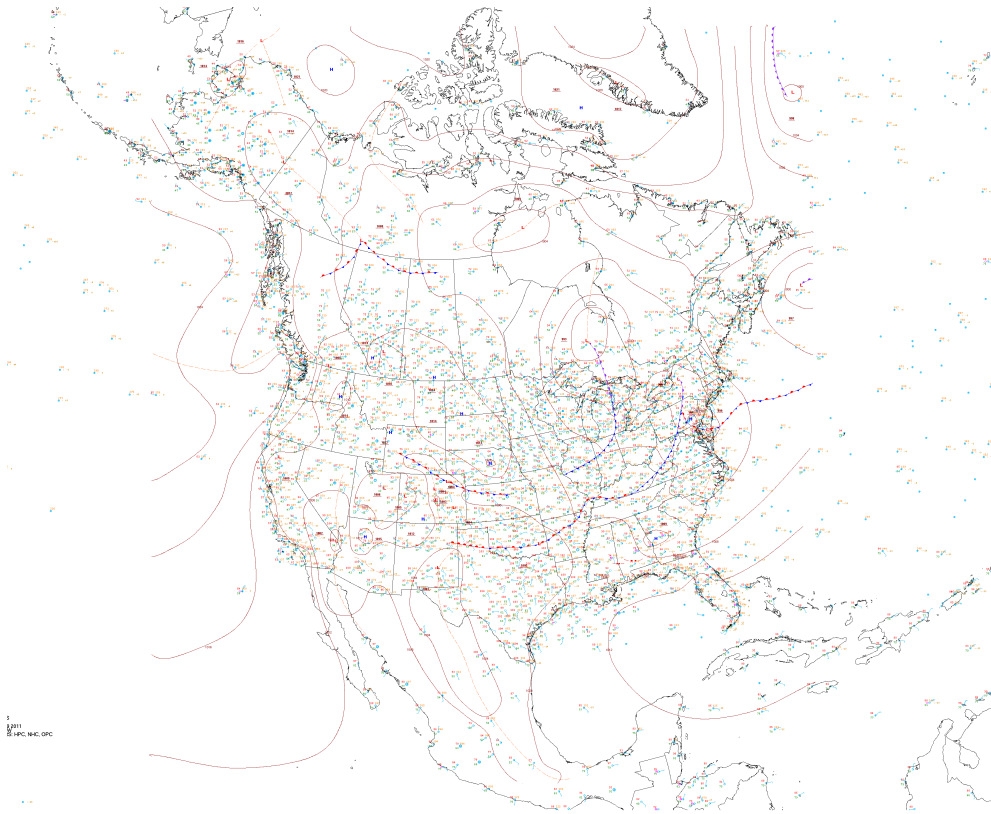


Figure S5: Surface analyses map of North America issued by the Hydrometeorological Prediction Center corresponding to nr10-1/10-2 precipitation event.

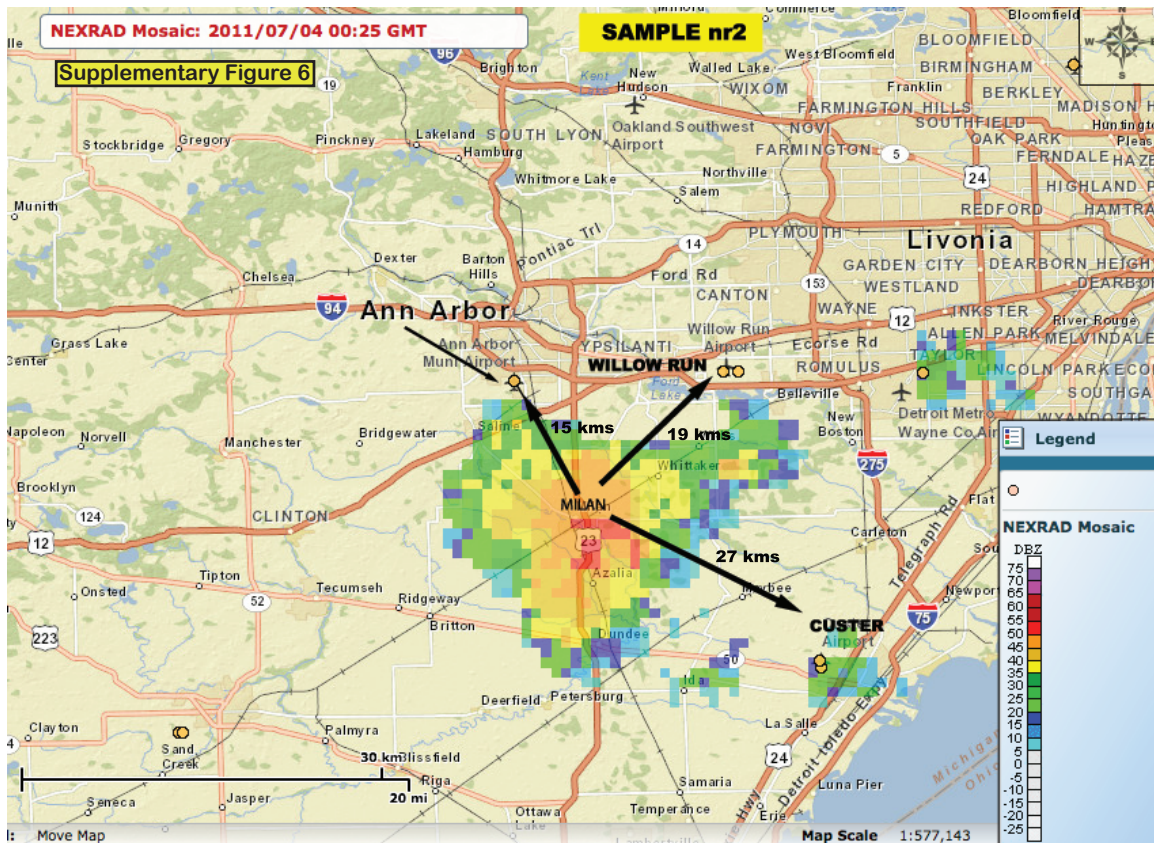


Figure S6: Doppler radar (NEXRAD) image for southeast Michigan at 00:25 UTC on July 4th, 2011. Location of hourly surface weather stations near Ann Arbor and Milan are also indicated (orange circles).

Supplementary Figure 7

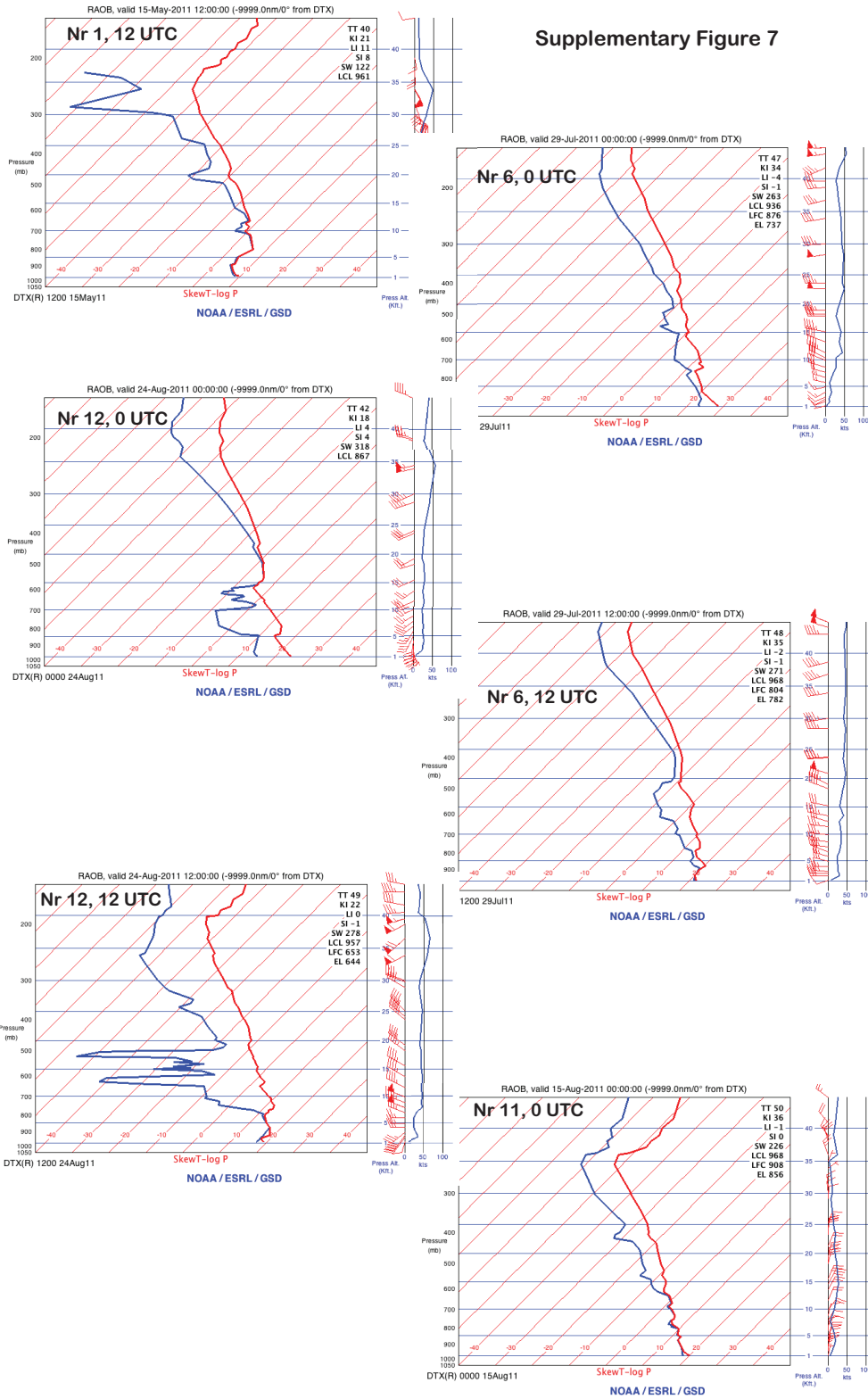


Figure S7: SkewT-log P plot of weather balloon measurements of temperature and dew point at Detroit, MI for samples nr1, 6, 11 and 12.

Supplementary Figure 8

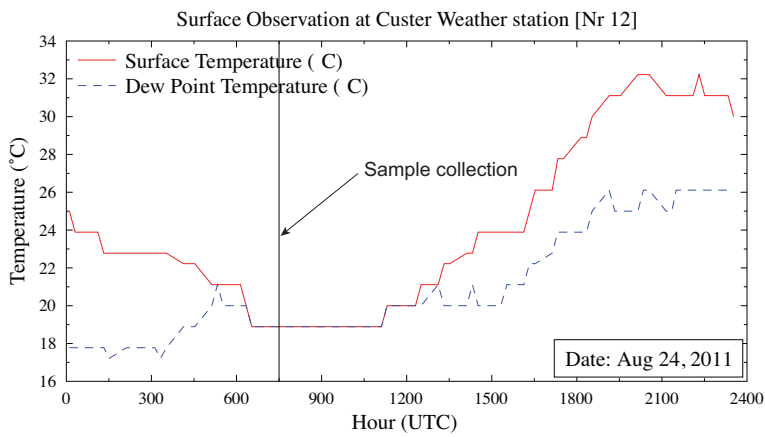
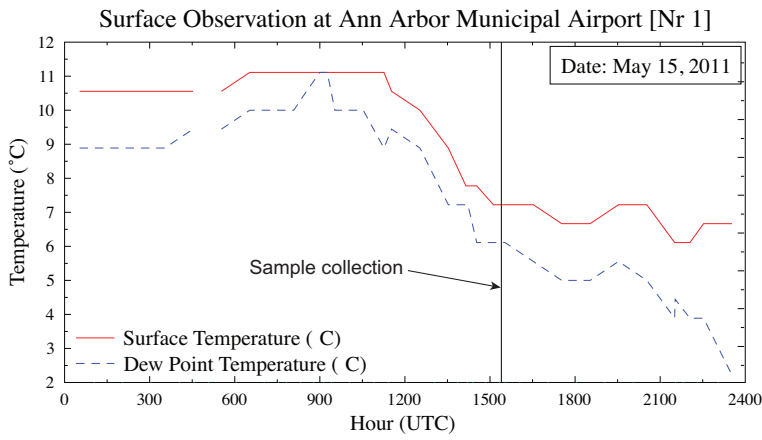
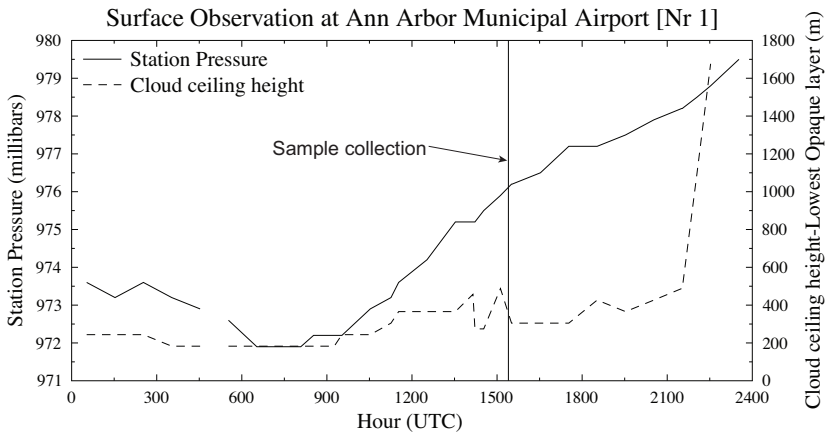


Figure S8: Plot of surface pressure, temperature, dew point and cloud ceiling height measurements for samples nr1 and nr12 measured at Ann Arbor and Custer weather stations respectively.

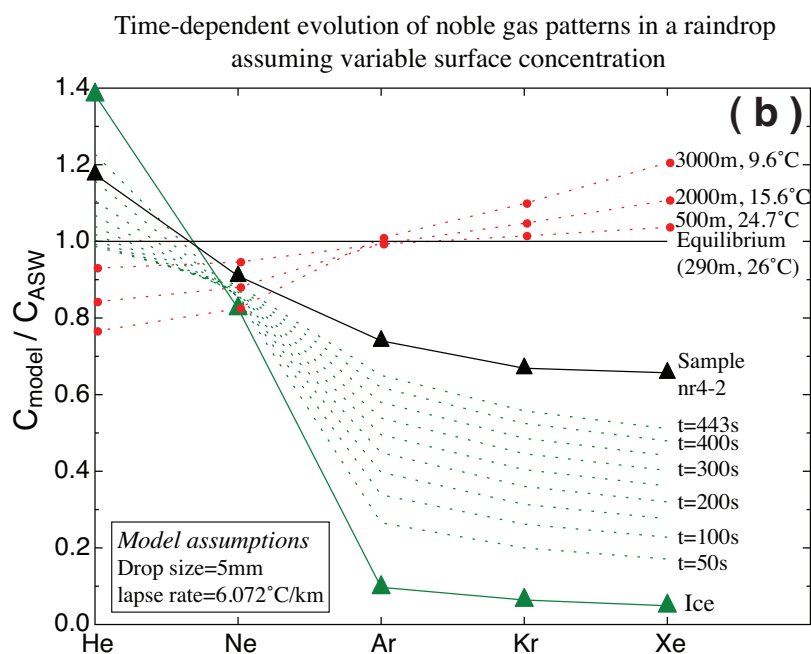
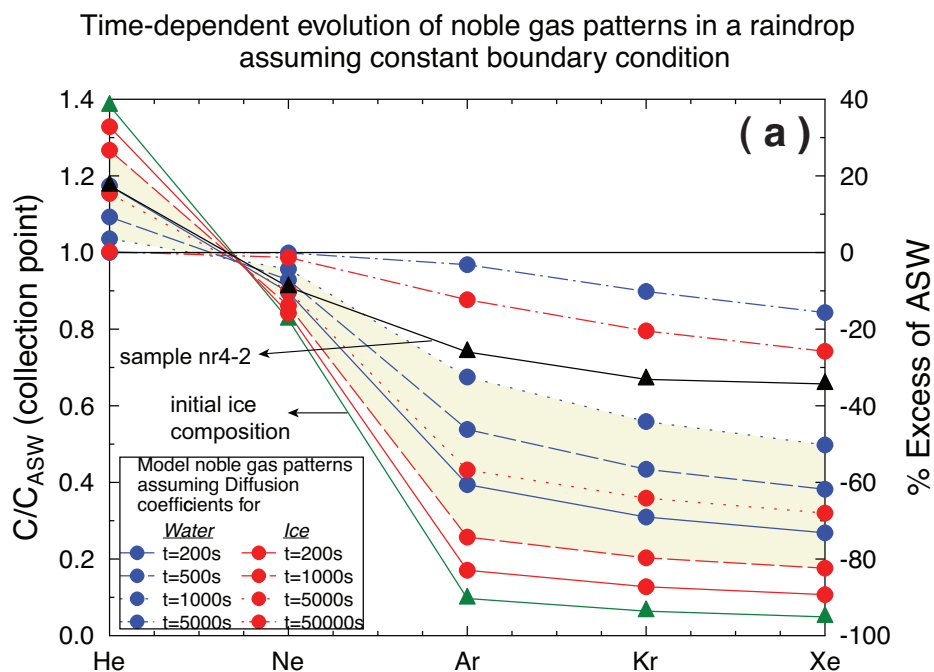


Figure S9. Comparison of measured rainwater noble gas patterns for sample nr4-2 (black markers) with the time dependent evolution of noble gas patterns within a raindrop of size 5mm starting from ice (green triangles). **(a)** Model noble gas patterns in a raindrop for various time 't' derived by assuming a constant equilibrium boundary condition and diffusion coefficients for ice (red markers) and liquid water (blue markers). Shaded region indicates domain of model rainwater patterns for t=1000s; **(b)** Model noble gas patterns in raindrop for various time 't' (green dashed lines) derived by assuming variable equilibrium boundary conditions (red dots) and liquid water noble gas diffusion coefficients.

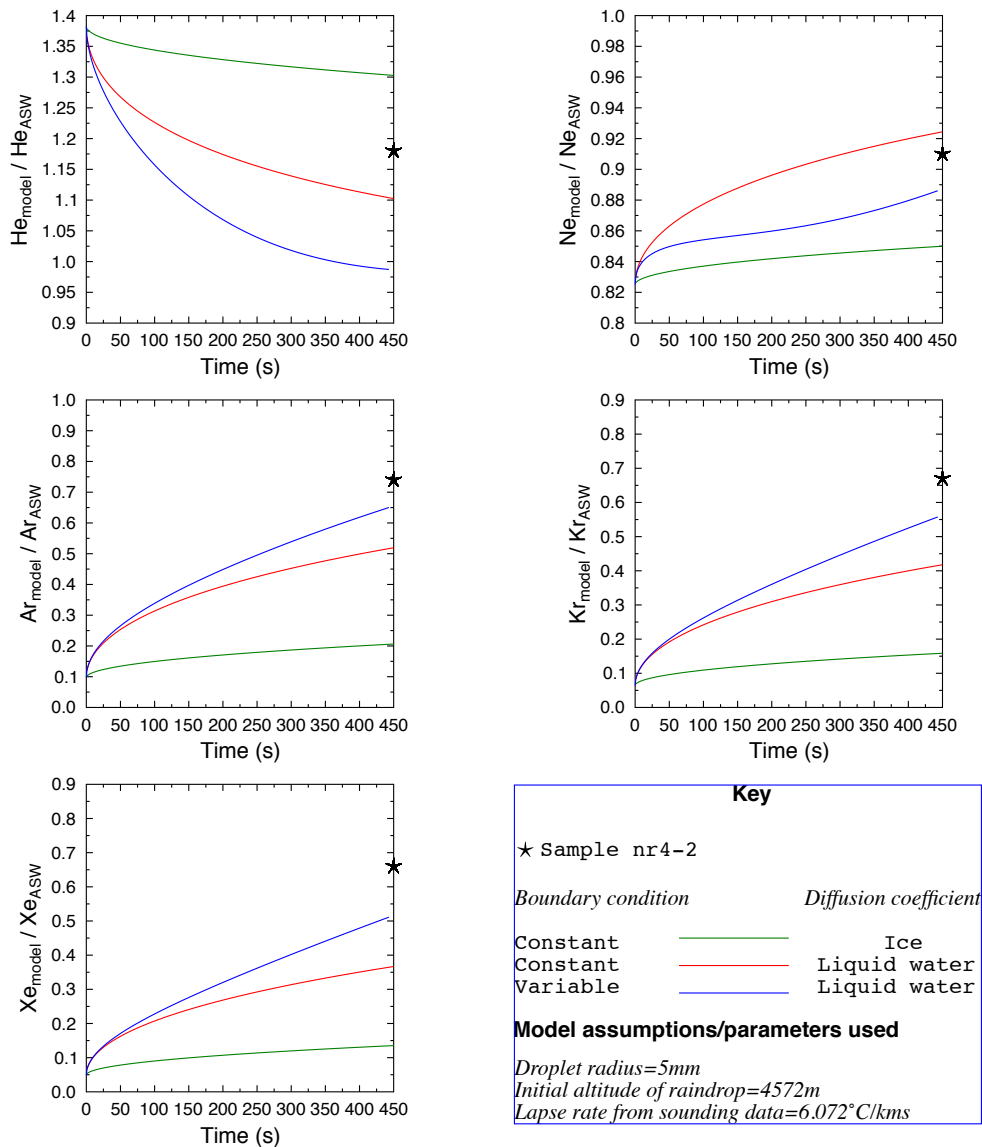


Figure S10. Comparison of the time evolution of noble gases within a raindrop of size 5mm derived by assuming boundary conditions and diffusion coefficients investigated in sections 2-4 of supplementary text3. These include (1) a constant equilibrium boundary condition of ASW at 0°C and noble gas diffusion coefficients in ice (green line); (2) constant equilibrium boundary condition of ASW at 0°C and noble gas diffusion coefficients in liquid water (red line); (3) varying equilibrium boundary condition as well as liquid water noble gas diffusion coefficients (blue line).

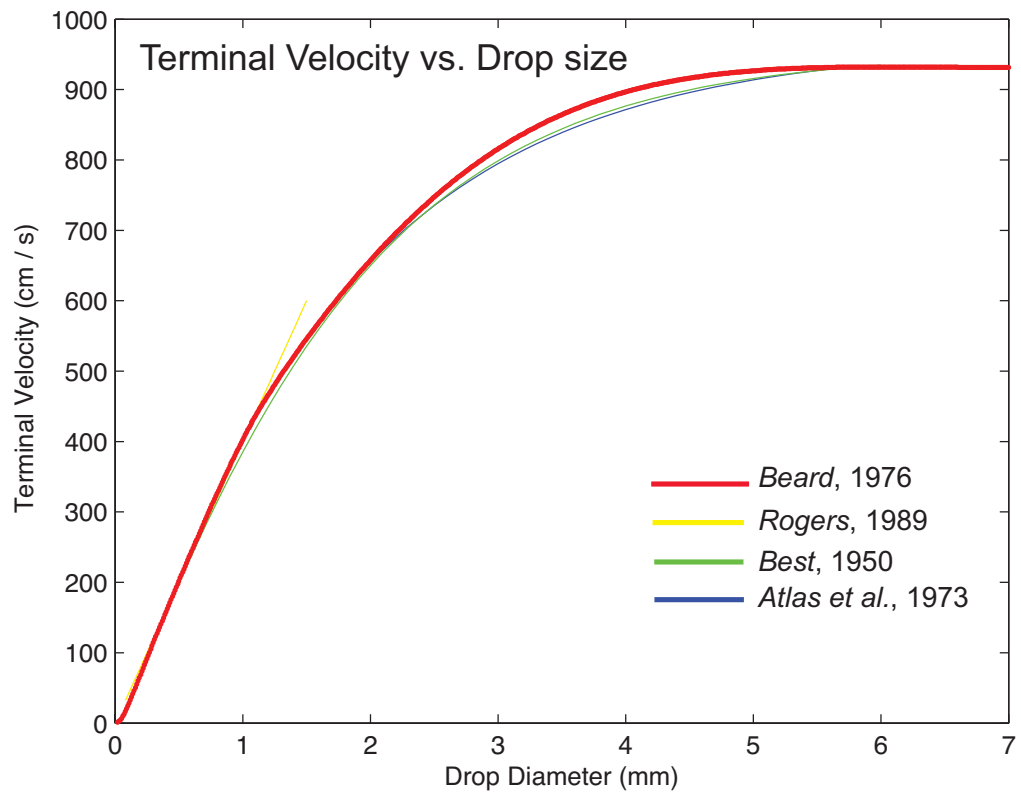


Figure S11: Terminal velocity of raindrops as a function of droplet size assuming multiple formulations.

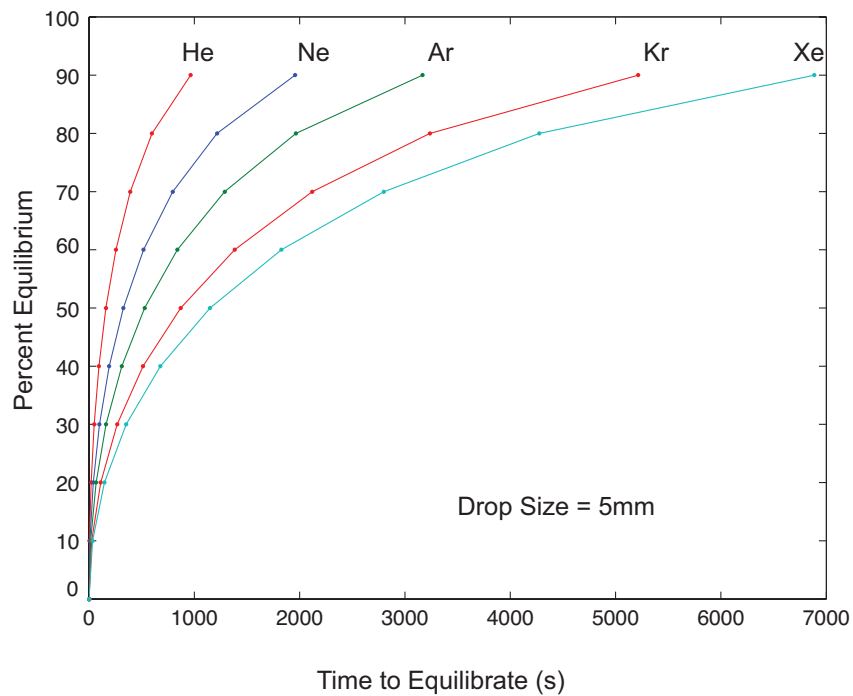
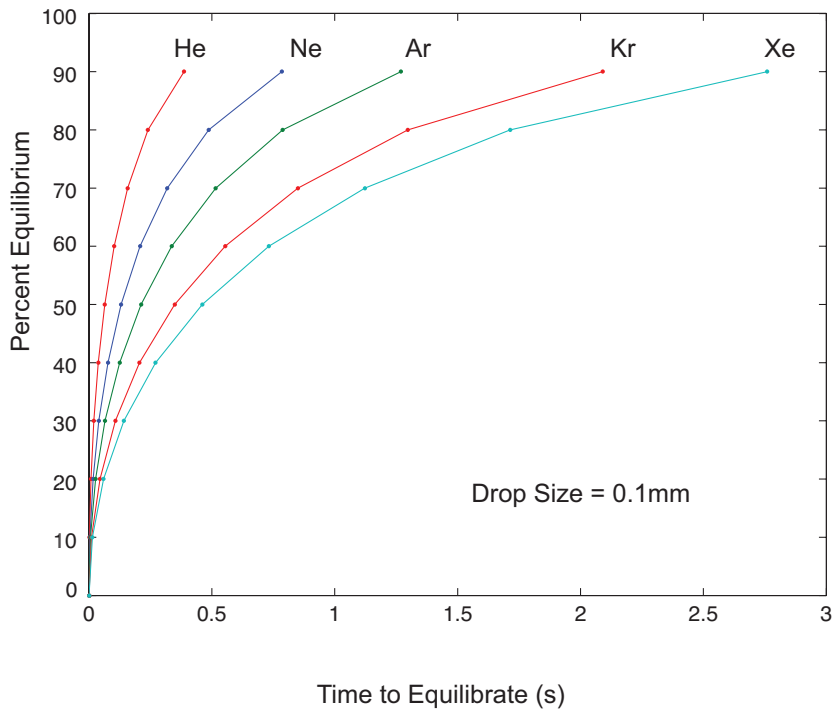


Figure S12: Time taken for noble gases to achieve diffusive equilibrium through mass transfer in/out of a raindrop of radius 0.1mm and 5mm.